Basic Studies on Modulation of Physiological Signals Generated by Fatty Acid Metabolisms for Anti-obesity and Anti-diabetes

January 2018

Hiroaki YASHIRO

Basic Studies on Modulation of Physiological Signals Generated by Fatty Acid Metabolisms for Anti-obesity and Anti-diabetes

A Dissertation Submitted to
the Graduate School of Life and Environmental Sciences,
the University of Tsukuba
in Partial Fulfillment of the Requirements
for the Degree of Doctor of Philosophy in Biological Science
(Doctoral Program in Biological Sciences)

Hiroaki YASHIRO

Table of Contents

Abstract 1

Abbreviations 4

General Introduction 6

Metabolic syndrome and metabolic domino 7
Beta cell dysfunction and insulin resistance 7
Physiological function of fatty acids 8
Modulation of fatty acids-mediated signals for therapeutic potentials 9

Chapter 1: D5D activity is important for the development of insulin resistance and obesity 10

Abstract 11
Introduction 11
Materials and Methods 13

Compound 13
Ethics Statement 14
Animals studies 14
In vitro enzyme assays for desaturase activities 14
In vitro cell-based assay for desaturase activities 15
Blood and tissue fatty acids measurement 16
Anti-obesity effects of D5D-inhibition in DIO mice 16
Oral glucose tolerant test 17
The effect of D5D-inhibition on energy expenditure in DIO mice 17
Indirect calorimetry test 17
Effects of D5D-inhibition on the expression of inflammation-related genes 18
RNA extraction and quantitative real-time polymerase chain reaction (RT-qPCR) 18
Statistics 19

Results 19

Effect of D5Dselective inhibitor on PUFA-desaturases in vitro 19
Anti-obesity effects of D5D-inhibition in DIO mice 20
Effect of D5D-inhibition on daily EE in DIO mice 21

Effects of D5D-inhibition on AA/DGLA ratio and gene expression in fat tissues 22
Discussion 24
Chapter 2: GPR40 mediated signal contributes to pancreatic hormone secretion 29
Abstract 30
Introduction 30
Materials and Methods 33
Cell culture 33
Chemicals 33
Static incubation assay 33
Islet perifusion analysis 34
Intracellular Ca^{2+} measurements 34
Quantification of mRNA expression of GPR40 and other receptor genes 35
Statistical analysis 36
Results 36
GPR40 signal on insulin and glucagon secretion in isolated rat islets 36
GPR40 signal on 1st and 2nd phases of insulin secretion at high glucose in perifused rat islets 37
GPR40 signal on $[Ca^{2+}]_i$ in individual cells within intact rat islets 37
Comparison of gene expression levels of GPR40, GLP-1R and SUR1 in human islets 38
GPR40 signal on insulin and glucagon secretion in isolated human islets 38
GPR40 signal on $[Ca^{2+}]_i$ in individual cells within intact human islets 39
Discussion 39
General Discussion 43
Acknowledgements 46
References 48
Tables 63
Table 1. Fatty acids mimetics proceeded into clinical trials 64
Table 2. Fatty acids composition of the high-fat diet (data are expressed as w/w%) 65
Table 3. In vitro IC_{50} values (nM) for fatty acid desaturases 66

Table 4. Sequences of TaqMan primers and probes 67
Table 5. Clinical profiles of islet donors 68
Table 6. Summary of the results of static incubation assay in human islets (from 4 organ donors) 69

Figures 70

Fig. 1 The concept of metabolic domino 71
Fig. 2 Changes of insulin secretion during the progression T2DM 72
Fig. 3 Classification and de novo fatty acids synthesis 73
Fig. 4 Biosynthesis pathway of n-6 polyunsaturated fatty acids 74
Fig. 5 Structure of D5D inhibitor; compound-326 74
Fig. 6 Effects of chronic treatment with D5D inhibitor on BW, calorie intake, and blood PD markers in DIO mice 75
Fig. 7 Effects of chronic treatment with D5D inhibitor on blood EPA and DHA levels in DIO mice 76
Fig. 8 Effects of chronic treatment with D5D inhibitor on plasma glucose and insulin during an OGTT, and HOMA-IR in DIO mice 77
Fig. 9 Effects of chronic treatment with D5D inhibitor on BW, calorie intake, and fat mass in DIO mice 78
Fig. 10 Effect of chronic treatment with D5D inhibitor on energy expenditure in DIO mice 79
Fig. 11 Effect of chronic treatment with D5D inhibitor on energy expenditure in DIO mice 80
Fig. 12 Effect of chronic treatment with D5D inhibitor on respiratory exchange ratio in DIO mice 81
Fig. 13 Effects of D5D inhibitor on BW and AA and DGLA levels within the blood as well as liver in DIO mice 82
Fig. 14 Effects of chronic treatment with D5D inhibitor on PD markers and gene expression in WAT in DIO mice 83
Fig. 15 Effects of chronic treatment with D5D inhibitor on blood and tissue EPA and DHA levels in HFD-fed mice 84
Fig. 16 Effects of D5D inhibitor on WAT gene expression in satellite DIO mice (Day32) 85
Fig. 17 Presumed mechanism of insulin secretion via GPR40 in pancreatic beta cell 86

Fig. 18 Effects of GPR40 agonist on insulin and glucagon secretion in rat islets 87
Fig. 19 Effect of GPR40 agonist on insulin secretion in perifused rat islets 88
Fig. 20 Effects of GPR40 agonist on the intracellular Ca^{2+} response of single β and α cells within intact rat islets 89
Fig. 21 Comparison of gene expression levels of GPR40, GLP-1R and SUR1 in human islets.....90
Fig. 22 Effects of GPR40 agonist on insulin and glucagon secretion in human islets.....91
Fig. 23 Effects of GPR40 agonist on the intracellular Ca^{2+} response of single β- and α-cells within intact human islets.....92
Fig. 24 Individual data of $[Ca^{2+}]_i$ response to 3 μM GPR40 agonist in three non-diabetic donors.....93

Abstract

Metabolic syndrome (MS) is a complex disorder defined by a cluster of interconnecting factors including obesity, diabetes, lipedema, hypertension, macro- and micro-vascular complications, and atherosclerosis. Although individual and genetic factors could influence the onset and severity of MS, the major causative factor for MS is the excessive intake of calorie, partly related to the western-style-diets which contains high amount of fat and carbohydrate spreading across the world.

Fatty acids are the major constituent of lipids, and utilized not only as an essential energy source for human health, but also contributes as a comportment of cell membrane, cholesterol ester, precursor of eicosanoids, ligand for nuclear receptors and G-protein coupled receptors (GPCR), as well as barrier function in epidermal. Therefore, I considered that basic research of fatty acids-mediated signals related to the onset of MS are worthy for the disease understanding and future drug discovery. Here, I report the physiological importance of delta-5-desaturase (D5D) mediated fatty acids metabolism on the obesity and insulin resistance (Chapter 1), and G-protein coupled receptor 40 (GPR40) signals on the glucose mediated insulin secretion from the pancreatic β-cells (Chapter 2).

Chapter 1: D5D activity is important for the development of insulin resistance and obesity.

D5D is an enzyme that metabolizes dihomo-γ-linolenic acid (DGLA; precursor to anti-inflammatory eicosanoids) to arachidonic acid (AA; precursor to pro-inflammatory eicosanoids). Thus, I used a D5D specific inhibitor, compound-326, to demonstrate the physiological importance of the enzyme on the development of MS using a high-fat diet induced obese (DIO) mouse model. *In vivo* D5D inhibition was confirmed by determining changes in blood AA/DGLA profiles. In DIO mice, chronic treatment with D5D inhibitor lowered insulin resistance and caused body weight loss without significant impact on cumulative calorie intake. Decreased macrophage infiltration into the adipose tissue was

suggested from mRNA analysis. In line with sustained body weight loss, increased daily energy expenditure was also observed following the inhibition of D5D.

Chapter 2: GPR40 mediated signal contributes to pancreatic hormone secretion

GPR40 is known as a GPCR which is activated by free fatty acids (FFA), as its natural ligands. To analyze the contribution of GPR40 signal on insulin and glucagon secretion, I evaluated the effect of synthetic GPR40 agonist, TAK-875, on hormone secretions using both human and rat isolated islets. In both species, stimulation of GPR40 signal enhanced insulin secretion in lines with the elevation of β-cell $[Ca^{2+}]_i$ in a glucose dependent manner. GPR40 stimulation did not affect glucagon secretion at both low and high glucose in human islets. These data indicate that GPR40 signal mainly influences insulin secretion from pancreatic β-cell in a glucose-dependent manner.

These studies reported here clearly support the idea that fatty acids and their metabolites play important roles in maintain the physiological functions, and pharmacological intervention to fatty acids-mediated signals would be a useful way to tackle the MS.

Abbreviations

AA	arachidonic acid
ALA	α-linolenic acid
AU	arbitrary units
AUC	area under the curve
BAT	brown adipose tissue
BSA	bovine serum albumin
CB1	cannabinoid receptor 1
CVD	cardiovascular disease
D5D	delta-5-desaturase
D6D	delta-6 desaturase
D9D	Delta-9 desaturase
DGLA	dihomo-γ-linolenic acid
DHA	docosahexaenoic acid
DIO	high-fat diet induced obese
DMSO	dimethyl sulfoxide
EE	energy expenditure
EPA	eicosapentaenoic acid
FFAs	free fatty acids
GAPDH	glyceraldehyde-3-phosphate dehydrogenase
GLP-1	Glucagon like peptide 1
GLU	glucose
GPCR	G-protein coupled receptors
GPR40	G-protein coupled receptor 40
HFD	high-fat diet
HOMA-IR	homeostasis model assessment of insulin resistance
KO mice	knock out mice
KRBH	Krebs-Ringer-bicarbonate HEPES buffer
LA	linoleic acid
LCFAs	Long-chain fatty acids
MC	methylcellulose
MCFAs	Medium-chain fatty acids
MS	Metabolic syndrome
ND	Normal diet
OGTT	oral glucose tolerance test
PCR	polymerase chain reaction
PD	pharmacodynamics
PUFA	Longer-chain polyunsaturated fatty acids
RER	respiratory exchange ratio
RIA	radioimmunoassay
SCFAs	Short-chain fatty acids
SUR1	sulfonylurea receptor 1
T2DM	type 2 diabetes
WAT	white adipose tissue

General Introduction

Metabolic syndrome and metabolic domino

Metabolic syndrome (MS) is a complex disorder defined by a cluster of interconnecting factors which lead to the life-threatening comorbidities, and the concept of "metabolic domino" has been proposed to capture the flow of events and chain reactions (Itoh 2006) (Fig. 1). Although the genetic predisposition could influence the vulnerability and progression of metabolic domino for each individual, lifestyle changes including sedentary workstyle in combination with over calorie intake are the first dominoes to fall, which lead to obesity and insulin resistance, followed by postprandial hyperglycemia, hypertension, and hyperlipidemia. These comorbidities could be a trigger of atherosclerosis, and once diabetes occurs, the domino for the impairment of insulin secretion has started. Progression of the atherosclerotic process can lead to cardiovascular events such as ischemic heart diseases or cerebrovascular disorders. Preclinical and clinical data indicate that treatments which inhibit the renin angiotensin system, such as angiotensin receptor blockers, can suppress the onset of diabetes (Aguilar and Solomon 2006). The inhibition of inflammation with thiazolidinedione can also block the sequence of events leading to cardiovascular outcomes, as was shown with pioglitazone in the Prospective Pioglitazone Clinical Trial in Macrovascular Events (PROactive) (Erdmann, Harding et al. 2016). Therefore, importance of lifestyle modification and primary prevention of the MS by medical care should be emphasized for the improvement of QOL for the patients.

Beta cell dysfunction and insulin resistance

Islets of Langerhans, small clusters of endocrine cells, makeup ~1–2% of the total pancreatic mass, and each islet is composed of multiple cell types, including insulin-producing β-cells, glucagon-producing α-cells, and several other less abundant cell types producing somatostatin, pancreatic polypeptide, and ghrelin (Hornblad, Cheddad et al. 2011). The amount of insulin secreted in response to metabolic demand is regulated by numerous factors, with proper sensing

of extra cellular nutrients including glucose and free fatty acids, as well as variety of hormones under the healthy condition. However, once peripheral insulin resistance is established, hyperinsulinemia is observed as a result of increased demand for insulin and this influences β-cells function and population markedly (Fig. 2). In addition, chronic exposure of β-cells to high blood glucose has detrimental effects on insulin synthesis and secretion, and affects survival by glucotoxicity, which in turn lead to hyperglycemia and form a vicious circle of continuous deterioration of β-cells dysfunction and apoptosis (Robertson, Harmon et al. 2004). Therefore, activation of glucose-stimulated insulin secretion may recover and prevent β-cells death via normalization of blood glucose for long-term benefits.

Physiological function of fatty acids

Short- and medium-chain fatty acids (SCFAs and MCFAs), along with more abundant long-chain fatty acids (LCFAs), are natural compounds present in both animal and plant tissues that participate in cell metabolism (Schonfeld and Wojtczak 2016). SCFAs and MCFAs are also known as important food constituents, where they are mostly in the form of triglycerides in some plant oils and milk (Schonfeld and Wojtczak 2016). Nevertheless, bacterial fermentation of amylase-resistant starch and non-starch polysaccharides in the gut is probably the most important source of SCFAs in humans and most mammalian species (Wong, de Souza et al. 2006) (Fig. 3). These fatty acids are not only energy sources, but also structural components of cell membranes (phospholipids) and second messengers (Kremmyda, Tvrzicka et al. 2011). Longer-chain polyunsaturated fatty acids (PUFA), including eicosapentaenoic acid (EPA), docosahexaenoic acid (DHA), and arachidonic acid (AA) are precursors of lipid mediators such as eicosanoids (prostaglandins, leukotrienes, thromboxanes), resolvins and neuroprotectins. The n-6 PUFA AA is the precursor of pro-inflammatory prostaglandins, leukotrienes, and related compounds, which have important roles in inflammation and in the regulation of

immunity. On the contrary, lipid mediators produced by EPA and DHA (Longer-chain n-3 PUFA; mainly found in oily fish) are considered as inflammation-resolving, and thus, fish oil has been characterized as anti-inflammatory. Moreover, these fatty acids and their metabolites play physiologically important roles as ligands of multiple nuclear receptors affecting gene expressions.

As for the relation to pancreatic β-cells, free fatty acids (FFA) are well known to enhance insulin secretion in the presence of elevated plasma glucose levels (Prentki, Vischer et al. 1992, Yaney and Corkey 2003). Plasma concentrations of FFA are elevated in the fasted state, and they play a role in the enhancement of the postprandial insulin response *in vivo* (Stein, Esser et al. 1996, Dobbins, Chester et al. 1998). Thus, fatty acids are involved in multiple pathways and play a major role in health.

Modulation of fatty acids-mediated signals for therapeutic potentials

Fatty acids and their mimetics are ligands of the fatty acids binding site in proteins that endogenously interact. Because fatty acids and their metabolites play important roles in maintain the physiological functions, there are numerous examples of successful fatty acids mimetics with therapeutic potentials in patients (Table 1) (Proschak, Heitel et al. 2017). With growing knowledge of physiological importance of fatty acids through the identification of novel signaling cascades and deorphanization of GPCRs, pharmacological intervention to fatty acids-mediated signals is expected to be a useful way to tackle the MS.

Chapter 1: D5D activity is important for the development of insulin resistance and obesity

Abstract

Obesity is now recognized as a state of chronic low-grade inflammation and is called as metabolic inflammation. Delta-5 desaturase (D5D) is an enzyme that metabolizes dihomo-γ-linolenic acid (DGLA) to arachidonic acid (AA). Thus, D5D-inhibition increases DGLA (precursor to anti-inflammatory eicosanoids) while decreasing AA (precursor to pro-inflammatory eicosanoids), and could result in synergistic improvement in the low-grade inflammatory state. Here, I demonstrate reduced insulin resistance and the anti-obesity effect of a D5D selective inhibitor (compound-326), an orally active small-molecule, in a high-fat diet induced obese (DIO) mouse model. *In vivo* D5D-inhibition was confirmed by determining changes in blood AA/DGLA profiles. In DIO mice, chronic inhibition of D5D lowered insulin resistance and caused body weight loss without significant impact on cumulative calorie intake. Decreased macrophage infiltration into adipose tissue was expected from mRNA analysis. Increased daily energy expenditure was also observed following chronic D5D-inhibition, in line with sustained body weight loss. These data indicate that chronic inhibition of D5D activity will be beneficial to prevent obese and diabetes in patients.

Introduction

Obesity is generally defined by an excessive fat accumulation, and is recognized as a pandemic nutritional disorder in both developing and developed countries (Chopra, Galbraith et al. 2002, Monteiro, Moura et al. 2004, Mendis, Lindholm et al. 2007, Haidar and Cosman 2011). The cause of obesity is usually attributed to a chronic imbalance between energy intake and energy expenditure (EE), and is the cause of complications such as type 2 diabetes (T2DM), dyslipidemia, and cardiovascular disease (CVD). Although individual and genetic factors could influence the onset and severity, the major causative factor for obesity is the excessive intake

of fat and carbohydrate, partly related to the western-style-diets spreading across the world (Pan, Malik et al. 2012). In western-style diets, PUFA comprise up to 20% of dietary fat, and linoleic acid (18:2, n-6, LA) and α-linolenic acid (18:3, n-3, ALA) usually contribute more than 95% of dietary PUFA intake, and the diets have low n-3/n-6 PUFA ratio (Simopoulos 2002, Simopoulos 2003, Glaser, Heinrich et al. 2010). PUFA are essential because they are not synthesized by the body and must be obtained through foods or supplementation (Covington 2004). Therefore, dietary intake and food sources of PUFA could influence the whole body PUFA compositions (Astorg, Bertrais et al. 2008).

Dietary LA is metabolized to dihomo-γ-linolenic acid (20:3, n-6, DGLA) by delta-6 desaturase (D6D; *Fads2*) followed by delta-5 desaturase (D5D; *Fads1*) to arachidonic acid (20:4, n-6, AA), which is a substrate for the synthesis of the pro-inflammatory eicosanoids (2 series of prostaglandins) (Fig. 4). An increase in whole desaturase activity, predicted by the enzyme product/enzyme substrate composition, was found in patients with essential hypertension (Russo, Olivieri et al. 1997), CVD (Domei, Yokoi et al. 2012), insulin resistance, obesity, and metabolic syndrome (Vessby 2003, Warensjo, Ohrvall et al. 2006, Inoue, Kishida et al. 2013). Therefore, an increased desaturase activity in combination with an n-6 rich environment may lead to a greater AA accumulation, thus favoring the synthesis of AA-derived mediators, which contribute to chronic inflammation.

It has been reported that the D5D/D6D dual-inhibitor, CP-24879, shows beneficial effects against increased intracellular lipid accumulation and inflammatory injury in hepatocytes (Lopez-Vicario, Gonzalez-Periz et al. 2014). The anti-inflammatory action of this dual inhibitor could mainly be caused by D6D inhibition, which will eventually cause a decrease in AA production. However, D6D inhibition has a more direct impact on reducing DGLA which have anti-inflammatory properties; DGLA is a precursor in the synthesis of prostaglandin E1 (PGE1) as well as 1 series of prostaglandins (Knapp, Oelz et al. 1978, Kirtland 1988, Zurier 1991). Therefore, contrary to the D5D/D6D inhibitor, pharmacological inhibition of D5D

activity could decrease AA synthesis as well as increase the abundance of DGLA, and synergistically ameliorate metabolic abnormalities by decreasing inflammatory signals, especially in the situation of high LA intake (e.g., Western-style diets).

Meanwhile, D5D is also involved in the metabolic pathway of n-3 PUFA; therefore inhibition of D5D may cause the decrease in *de novo* synthesis of eicosapentaenoic acid (20:5, n-3, EPA) and docosahexaenoic acid (22:6, n-3, DHA) from dietary ALA. Increasing evidence suggests that these n-3 PUFA exert health benefits (Swanson, Block et al. 2012, Dyall 2015); thus D5D-inhibition may cause some negative impacts on these beneficial effects of n-3 PUFA. On the other hand, recently published paper indicated that D5D knock out (KO) mice showed the phenotype of decreased body fat, improved glucose tolerance, lower fasting serum levels of insulin, cholesterol, and triglycerides compared to wild type mice without abnormal findings (Baugh, Pabba et al. 2015, Powell, Gay et al. 2016); therefore, D5D-inhibition could be a therapeutic target for metabolic disease.

Here, I report the therapeutic potential of D5D-inhibition on obesity and insulin resistance using D5D selective inhibitor as a pharmacological tool.

Materials and Methods

Compound

The D5D selective inhibitor, 2-(2,2,3,3,3-Pentafluoropropoxy)-3-[4-(2,2,2-trifluoroethoxy) phenyl]-5,7-dihydro-3H-pyrrolo[2,3-d]pyrimidine-4,6-dione, compound-326 (WO 2010087467A1), was synthesized in Chemical Development Laboratories at Takeda Pharmaceutical Company Limited (Suzuki, Fujimoto et al.). Sibutramine hydrochloride monohydrate was purchased from Wako Pure Chemicals (Osaka, Japan). For *in vivo* studies,

compounds were suspended in 0.5 w/v% methylcellulose (MC; Wako, Osaka, Japan) solution and administered orally.

Ethics Statement

The care and use of the animals and the experimental protocols used in this research were approved by the Experimental Animal Care and Use Committee of Takeda Pharmaceutical Company Limited, Japan and the Guide for the Care and Use of Laboratory. During the experimental procedure, I monitored animals every day. Animal conditions were assessed by any symptoms including abnormal behavior, severe anorexia, skin ulceration, and diarrhea. No abnormal findings were noted, and all the mice were well-care and healthy during the experimental procedures. For hepatic-microsomes preparation, rats were sacrificed by decapitation. At the end of all the experiments, mice were sacrificed by exsanguination under pentobarbital anesthesia.

Animals studies

In this report, I performed 3 independent studies in DIO mice to characterize anti-obesity effects of the D5D-inhibition. Male C57BL/6J mice were obtained from Charles River Laboratories (Yokohama, Japan) or CLEA Japan (Osaka, Japan). The mice were fed a laboratory chow and water *ad libitum* and housed in a 12-h light/dark cycle. Compound or vehicle was administered once daily between 15: 00-19:00 by oral gavage. Body weight (BW) and food intake were monitored throughout the experiment.

In vitro enzyme assays for desaturase activities

Delta-9 desaturase (D9D) is a rate-limiting enzyme in the biosynthesis of monounsaturated fatty acids, and it was reported that D9D KO mice demonstrate resistance to diet-induced obesity, increased insulin sensitivity, and increased metabolic rate (Ntambi, Miyazaki et al.

2002). Therefore, I also confirmed that D5D inhibitor, compound-326, has no effect on D9D activity. Inhibitory activity of compound-326 on rat D5D, D6D, and D9D was evaluated using hepatic microsomes prepared from SD rats (CLEA, Japan) as described previously (Miyahisa, Suzuki et al. 2016). Assays were performed in a total volume of 30 μL in 96-well plates in a buffer containing 100 mM $NaHPO_4$, 150 mM KCl, 10 mM NaF, 1.5 mM glutathione, 3 mM $MgCl_2$, 1 mM NADH, 3 mM ATP, 0.3 mM CoA-SH, and 0.1% fatty acid free bovine serum albumin (BSA, Sigma, St. Louis, MO); and 0.1 μCi/well of [^{14}C] DGLA or [^{14}C] linoleic acids (ARC, St. Louis, MO) were used as substrates for measuring D5D and D6D activities, respectively. After pre-incubation of the test compound with rat liver microsomes (final 1.0 mg/mL) for 5 min, the reaction was started by the addition of NADH, ATP, and the substrates, and the reaction mixture was incubated for another 120 min at room temperature. For D9D assay, [^{14}C] stearoyl-CoA (PerkinElmer, Waltham, MA) was used in the absence of NADH, ATP, and CoA-SH, and D9D enzyme reaction was performed for 30 min. The reactions were then terminated by the addition of 0.63 N NaOH. After overnight incubation at 55°C for saponification, the solvent extraction of fatty acids was carried out as described previously (Bligh and Dyer 1959). The chloroform layer was spotted on a reverse phase TLC plate, RP-18 F254s (Merck Millipore, Darmstadt, Germany), and then developed with acetonitrile: water: acetic acid (95:4.5:0.5). Detection was carried out using BAS-5000 (Fujifilm, Tokyo, Japan). The images were digitalized using Multi Gauge ver. 2.3 (Fujifilm) and IC_{50} values were determined using the conversion ratio from the radioactive substrates (20:3n6, 18:2n6 and 18:0) to the products (20:4n6, 18:3n6 and 18:1n9).

In vitro cell-based assay for desaturase activities

HepG2 cells were seeded in 96-well cell culture plates at 100,000 cells/well and incubated overnight in DMEM supplemented with 10% fetal bovine serum, 100 U/mL penicillin, and 100 μg/mL streptomycin in 5% CO_2 at 37°C. The cells were washed twice with 200 μL of PBS and

incubated with the test compounds in DMEM with 0.1 % fatty acid free BSA for 30 min. Then, 0.1 μCi/well of [^{14}C]-labeled DGLA, linoleic acid, and stearic acid (ARC, St. Louis, MO) were added for each desaturase assay. After incubation for 3 h at 37°C, the cells were washed 3 times with 200 μL of PBS to remove [^{14}C]-labeled substrates in the medium and 0.63 N of NaOH was added to saponify fatty acids. Radioactive substrates and products were extracted, separated, and analyzed using the method as described above.

Blood and tissue fatty acids measurement

Fatty acids were extracted from blood and tissues by adding hexane-isopropanol-butylated hydroxytoluene (60:40:0.01, v/v/w). Samples were vortexed for 30 min. The hexane phase was removed and evaporated to dryness under nitrogen stream and vacuum. Dried samples were dissolved in methanol and analyzed by HPLC.

Anti-obesity effects of D5D-inhibition in DIO mice

Mice were fed a high-fat diet (HFD) that has 60% kcal from fat and contains 0.09% (w/w) AA (D12492; Research diets, Inc., see table 2 for fatty acid profile) from 5 weeks of age, and they were divided into 5 groups (7 animals per group) at 11 weeks of age based on BW and daily food intake. In this experiment, 30 mg/kg sibutramine, a serotonin-dopamine reuptake inhibitor, was used as a positive control for anti-obesity effects. Mice were orally administered D5D selective inhibitor at doses of 0.1, 1, and 10 mg/kg, sibutramine at a dose of 30 mg/kg, or vehicle for 6 weeks. After 6 weeks, blood concentrations of DGLA and AA under non-fasting condition were evaluated as pharmacodynamics (PD) markers, and oral glucose tolerance test (OGTT) was performed.

Oral glucose tolerant test

On the last day of the experiment, mice were given an oral glucose load (2 g/kg) after overnight fasting. Blood samples were collected at specified time points of 0 (pre-glucose/fasting glucose levels), 10, 30, 60, and 120 min post glucose load for the determination of plasma glucose as well as insulin levels. Plasma glucose was enzymatically measured with auto-analyzer 7180 (Hitachi High-Technologies Corporation, Tokyo, Japan). Plasma insulin was measured with mouse insulin ELISA kit (Shibayagi, Gunma, Japan). The total area under the glucose curve was determined from time 0 to 120 min ($AUC_{0–120\ min}$) after glucose administration. Homeostasis model assessment-insulin ratio (HOMA-IR) was calculated using the formula: [(fasted PG: mg/dL)×(fasted insulin; μU/mL)×26/405] (Matthews, Hosker et al. 1985).

The effect of D5D-inhibition on energy expenditure in DIO mice

To evaluate the effect on daily EE, DIO mice fed a HFD that has 41% kcal from fat and contains no AA (D12079B; Research diets, Inc., see table 2 for fatty acids composition) for 50 weeks were used. At 55 weeks of age, DIO mice were divided into two weight-matched groups (7 animals per group) and treated with vehicle or 10 mg/kg D5D inhibitor for 11 weeks. The dose of D5D inhibitor, 10 mg/kg, was selected that showed clear BW reduction in the previous study. Indirect calorimetry test was performed on day1, 8, 15, 21, and 56 during the study. Daily EE was analyzed using ANCOVA with body mass as covariate (Tschop, Speakman et al. 2012). After the treatment period, mice were sacrificed and fat tissues were harvested to evaluate the weights.

Indirect calorimetry test

Energy metabolism was evaluated using an Oxymax indirect calorimetry system (Columbus Instruments, Columbus, OH). Mice were individually housed in the chamber with a 12-h

light/dark cycle. VO_2 and VCO_2 rates were determined with the following Oxymax system settings: air flow, 0.6 L/min; sample flow, 0.5 l/min; settling time, 10 min; and measuring time, 1 min. The system was calibrated against a standard gas mixture to measure O_2 consumed (VO_2, mL/kg/h) and CO_2 generated (VCO_2, mL/kg/h). Metabolic rate (VO_2) and respiratory exchange ratio (RER; ratio of VCO_2/VO_2) were evaluated over a 24-h period. EE was calculated as the product of the calorific value of oxygen (3.815+1.232×RER) and the volume of O_2 consumed.

Effects of D5D-inhibition on the expression of inflammation-related genes

Mice fed a HFD that has 41% kcal from fat and contains no AA (D12079B; Research diets, Inc.) from 5 weeks of age were divided into 2 groups at the age of 8 weeks (8 animals per group), and were administered 10 mg/kg D5D inhibitor or vehicle for 6 weeks. After the treatment period, mice were sacrificed and epididymal and subcutaneous fats were harvested for mRNA analysis. Nine animals maintained on a standard chow (CE2, CLEA Japan, Osaka) were used as control.

RNA extraction and quantitative real-time polymerase chain reaction (RT-qPCR)

Total RNA was extracted and purified using RNeasy Mini Kit (QIAGEN, USA). First-strand cDNA was synthesized using High Capacity cDNA Reverse Transcription Kits (Thermo Fisher, USA). The mRNA levels were quantified by an ABI Prism 7900 TaqMan PCR system (Thermo Fisher, USA) according to the manufacturer's instruction using TaqMan® Universal PCR Mastermix with the primer-probe sets of TaqMan Gene Expression Assays (Thermo Fisher, USA) for the following genes: *Ccl2* (chemokine (C-C motif) ligand 2; Mm99999056_m1), *Cd68* (CD68 antigen; Mm03047343_m1), *Adgre1* (adhesion G protein-coupled receptor E1 ; Mm00802529_m1), *Tnf* (tumor necrosis factor; Mm00443258_m1), *Il6* (interleukin 6; Mm99999064), *Lep* (leptin; Mm00434759_m1), *Adipoq* (adiponectin; Mm00456425_m1), *Fads2* (D5D; Mm00517221_m1), *Fads1* (D6D; Mm00507605_m1), *Ucp1* (uncoupling protein

1; Mm00494069_m1), *Elovl3* (elongation of very long chain fatty acids 3; Mm00468164_m1), *Cidea* (cell death-inducing DNA fragmentation factor, alpha subunit-like effector A; Mm00432554_m1), *Otop1* (otopetrin 1; Mm00554705_m1), and *Rplp0* (ribosomal protein, large, P0; forward; 5'-CCCTGAAGTGCTCGACATCAC-3', reverse; 5'-GCGCTTGTACCCATTGATGA-3', probe (VIC-5'→3'-TAMRA); 5'-CCCTGCACTCTCGCTTTCTGGAG-3'). The *Rplp0* mRNA level was used as a reference and relative transcript levels were calculated with the comparative Ct method ($2^{-\Delta\Delta CT}$) (Applied Bio-systems).

Statistics

Results are expressed as mean ± *SEM*. Statistical analysis between two groups was assessed by Aspin-Welch test or Student's *t*-test depending on equal or unequal variances. For these analyses, a *p*-value less than 0.05 was considered significant. The dose-dependent effect of D5D inhibitor vs. vehicle was evaluated by the one-tailed Williams' test or Shirley-Williams test depending on equal or unequal variances and a *p*-value less than 0.025 was considered significant.

Results

Effect of D5Dselective inhibitor on PUFA-desaturases *in vitro*

Here I used an orally bioavailable D5D selective inhibitor, compound-326, as a research tool. (Fig. 5) (Suzuki, Fujimoto et al.). As shown in table 3, compound-326 has a potential to inhibit D5D activity (IC_{50}=72 and 22 nM for rat and human D5D, respectively); whereas, almost no inhibition was observed on both rat and human D6D activities. I also confirmed that compound-326 has no effect on D9D activity.

Anti-obesity effects of D5D-inhibition in DIO mice

To examine the anti-obesity potential of D5D-inhibition, I administered D5D inhibitor at doses of 0.1, 1, and 10 mg/kg orally to DIO mice for 6 weeks. As shown in Fig. 6A, mice treated with vehicle only showed increased BW during the experiment, and the sibutramine group showed transient and potent decrease in food intake from day 1, followed by a rebound. The sibutramine group showed potent BW loss for a week, but BW increased in line with increased food intake. On the other hand, the group treated with 10 mg/kg of D5D inhibitor showed gradual decrease in BW; however, lower doses were not effective. Unlike sibutramine, daily calorie intake was not altered significantly due to the administration of D5D inhibitor at all doses; although slight decrease was observed at a dose of 10 mg/kg (Fig. 6B). No abnormal findings such as behavioral changes, diarrhea, or steatorrhea were observed by D5D-inhibition. To confirm *in vivo* D5D-inhibition, I determined blood AA and DGLA levels after 6 weeks of treatment. D5D inhibitor decreased blood AA in conjunction with increased blood DGLA, in a dose-dependent manner (Fig. 6C); therefore, the AA to DGLA ratio decreased significantly (Fig. 6D). Since there was a large difference in BW loss between 1 and 10 mg/kg of D5D inhibitor, I analyzed statistical difference in the blood AA/DGLA profiles between these two doses. Although the changes were small, statistical difference was observed between the doses. Sibutramine treatment slightly but significantly decreased both blood AA and DGLA levels as well as the AA to DGLA ratio, which could be correlated to the reduction in BW. Because D5D is also active in the metabolic pathway of n-3 PUFA, I evaluated the effects of D5D-inhibition on blood levels of EPA and DHA. As shown in Fig. 7, both n-3 PUFA were decreased by D5D inhibitor in a dose dependent manner. An OGTT was performed after 6-week treatment, and glucose clearance was found to be improved by D5D inhibitor in a dose-dependent manner (Fig. 8A and B), while no change was observed in the insulin levels (Fig. 8C). In line with improved glucose clearance, HOMA-IR, an insulin resistance index, was also

decreased by D5D inhibitor in a dose-dependent manner (Fig. 8D). Treatment with sibutramine significantly improved HOMA-IR, but glucose clearance, as measured by the OGTT, was not improved.

Effect of D5D-inhibition on daily EE in DIO mice

As indicated above, D5D-inhibition prevented obesity and ameliorated insulin resistance without any appreciable decrease in calorie intake. Hence, I next confirmed the amelioration of obesity by D5D-inhibition using established DIO mice that had been fed a HFD for 50 weeks before the experiment. There was no significant difference between the groups in BW prior to treatment (vehicle; 50.4 ± 5.1g, 10 mg/kg D5D inhibitor; 50.9 ± 3.8g). Consistent with the results obtained in the HFD-fed growing DIO model, chronic D5D-inhibition caused sustained and significant BW reduction from day 21 until day 77 (Fig. 9A). Intriguingly, while no appreciable change in cumulative calorie intake was observed upon D5D-inhibition, daily calorie intake was slightly decreased until day 21, followed by a trend toward increase (Fig. 9B). Mice treated with D5D inhibitor for 11 weeks showed marked decrease in the white adipose tissue (WAT) depot mass compared to vehicle-treated mice; mesenteric fat ($p \leq 0.05$), subcutaneous and epididymal fat ($p \leq 0.01$) (Fig. 9C). Since observed loss in calorie intake could not explain remarkable weight loss, changes in EE were monitored on days 1, 8, 15, 21, and 56, and daily variations are shown in Fig. 10. To evaluate the effect on EE, general linear model analysis was applied on each point. On days 1 and 8, no difference was observed between vehicle- and D5D inhibitor-treated groups when daily EE (kcal/day) was plotted against body mass (Fig. 11A and B). However, on day 15, daily EE lays on two separate lines relative to body mass (Fig. 11C), and these changes demonstrate that EE was increased by D5D-inhibition independent of the decreased BW (Speakman 2013). Moreover, the difference between these lines became more apparent on days 21 and 56, consistent with the amelioration

of obesity (Fig. 11D and E). D5D-inhibition lowered RER relative to vehicle-treated mice through the study, but the change did not reach significance (Fig. 12).

Effects of D5D-inhibition on AA/DGLA ratio and gene expression in fat tissues

To further characterize the effects of the D5D-inhibition, I evaluated changes in the expression of genes related to inflammation and metabolic processes in fat tissues. DIO mice treated with 10 mg/kg D5D inhibitor showed a resistance to obesity, and 6-week treatment significantly decreased BW compared to vehicle treatment (Fig. 13A and B). In addition, a decrease in the AA to DGLA ratio in the blood, as a consequence of decreased AA and increased DGLA, was confirmed in the D5D-inhibited group (Fig. 13C and D). I also evaluated AA and DGLA contents in the liver (Fig. 13E and F) as well as in epididymal fat tissue (Fig. 14A and B). In HFD-fed DIO mice, the AA to DGLA ratio in the liver was significantly decreased compared to normal diet (ND)-fed mice; HFD-feeding increased both DGLA and AA, and the increase in DGLA overcame the increase in AA in the liver (Fig. 13E and F). The pattern of AA and DGLA changes in the liver are the same as in the blood (Fig. 13C and D). On the other hand, the AA to DGLA ratio in epididymal fat was significantly increased in HFD-fed DIO mice compared to ND-fed mice; DGLA was significantly decreased by HFD-feeding, while AA was increased in epididymal fat tissue (Fig. 14A and B). These results indicate that changes in the AA to DGLA ratio, namely the D5D activity, in metabolically unhealthy conditions could be different in tissues, and its changes in the blood seem to reflect the liver conditions. However, D5D-inhibition significantly decreased the AA to DGLA ratio in both tissues, and the change in AA and DGLA in the blood could be a reliable PD marker to confirm the D5D-inhibition in tissues. I also evaluated the effect of D5D-inhibition on EPA and DHA levels in blood and tissues (Fig. 15); however, liver EPA level in D5D-inhinited DIO mice and DHA level in adipose tissue of DIO mice were not measurable due to the analytical detection limit. ND-fed mice showed much higher levels of EPA and DHA compared to HFD-

fed DIO mice possibly due to the difference in the PUFA composition of the meal; CE2 diet contains fish-meal, while HFD do not contain any EPA or DHA (Table 2). As expected, D5D-inhibition significantly decreased both n-3 PUFA in blood, liver, and adipose tissue.

In epididymal fat, the expression levels of *Ccl2*, *Cd68*, and *Adgre1* were significantly higher in HFD-fed DIO mice compared to these in ND-fed mice (Fig. 14C). And these genes were decreased by chronic D5D-inhibition; while significant effect of D5D-inhibition was only observed in *Ccl2*. As for *Tnf* and *Il6* genes, up-regulation of these genes were not clearly observed in the HFD-fed DIO model; *p* value of *Tnf* and *Il6* between HFD-fed DIO and ND-fed mice are 1.00 and 0.46, respectively. Effects of D5D-inhibition on these inflammation-related genes in epididymal fat were also evaluated using satellite DIO mice that had been treated with compound-A or vehicle for 32 days (Fig. 16). At the intermediate point, D5D-inhibition significantly decreased gene expression levels of *Ccl2*, *Cd68*, *Adgre1*, and *Il6* (Fig. 16B), while no significant BW loss was observed (Fig. 16A). D5D-inhibition also decreased epididymal *Lep* and *Adipoq* mRNAs which were significantly increased in HFD (Fig. 14C); the effects did not reach statistical difference in *Adipoq* mRNA (p=0.08). HFD-fed DIO mice showed significantly lower D5D and D6D mRNA expression in epididymal fat, and D5D-inhibition upregulated their expression. In subcutaneous fat, no induction of beige fat cell-selective genes, including *Ucp1*, *Cidea*, *Elovl3*, and *Otop1* were detected by D5D-inhibition (Fig. 14D). *Lep* mRNA in subcutaneous fat was decrease by D5D-inhibition, but the difference did not reach statistical significance (*p*=0.08).

Discussion

Considering the physiological importance of PUFA, D5D and D6D activities are likely regulating a number of metabolic and inflammatory pathways. In addition, the use of product-to-precursor ratio as surrogate to estimate desaturase activity is well established, and this method has been used in epidemiological studies (Vessby, Gustafsson et al. 2002). In such studies, D6D has received much more attention compared to D5D with respect to metabolic disorders, because data demonstrated strong positive correlations between increased D6D activity and insulin resistance, BMI, and T2DM, while D5D activities showed negative correlation (Warensjo, Ohrvall et al. 2006, Steffen, Vessby et al. 2008, Warensjo, Rosell et al. 2009, Park, Hasegawa et al. 2010, Kroger, Zietemann et al. 2011, Saito, Okada et al. 2013). Additionally, metabolic benefits of D6D-inhibition were also predicted from the results that D6D KO mice exhibited resistance against HFD-induced obesity (Stoffel, Hammels et al. 2014).

Regarding D5D, Powell *et al*. recently reported that D5D KO mice showed lean phenotype with improved glycemic control and decreased development of atheromatous plaque under HFD-feeding (Powell, Gay et al. 2016). Hence, although there is no clear human evidence available to support the metabolic benefits of D5D-inhibition, the concept is similar to D6D-inhibition; it will block the supply of AA, which is required for the production of pro-inflammatory eicosanoids. In addition, D5D-inhibition increases the abundance of DGLA, which is a known precursor for anti-inflammatory eicosanoids. Thus, pharmacological inhibition of D5D activity may synergistically ameliorate metabolic abnormalities by decreasing inflammatory signals due to the decrease in AA/DGLA ratio.

In the first study, I found that 6-week D5D-inhibition prevented HFD-induced obesity with a slight decrease in daily calorie intake; although it was not enough to explain the remarkable change in BW. Here, I used sibutramine, which produces anorexigenic effects by

norepinephrine, serotonin, and dopamine reuptake inhibition, as a positive control for anti-obesity effect. Intriguingly, although both sibutramine and D5D inhibitor showed potent loss in BW, D5D inhibitor did not decrease food intake as sibutramine.

As indicated above, fatty acid product-to-precursor ratio in the blood has been widely used to estimate PUFA desaturase activity (Vessby, Gustafsson et al. 2002); hence, I used changes in the blood AA to DGLA ratio to estimate the inhibition of D5D activity by the test compound. As expected from *in vitro* studies, blood samples from mice with D5D-inhibition showed decreased AA and increased DGLA in a dose-dependent manner, and these results indicate that compound-326 has a potential to inhibit D5D activity *in vivo*. Although a significant change in BW could only be observed at a higher dose (10 mg/kg) having a high impact on blood AA and DGLA levels, improvement in glucose tolerability and insulin sensitivity were observed from dose of 1 mg/kg without a significant decrease in BW. These results suggest that near complete inhibition of D5D may be required for loss of BW, while partial inhibition may be enough to improve insulin sensitivity.

I also evaluated anti-obesity effect of D5D inhibition in established DIO mice, and chronic treatment with 10 mg/kg D5D inhibitor reduced BW, but had a lower effect on calorie intake. While short-term D5D inhibition did not increase EE, chronic administration increased EE in line with BW reduction. These results suggest that increased EE by D5D inhibition may require modified cellular AA and DGLA profiles, which would require a longer period.

Although D5D inhibition could exert an influence on AA and DGLA profiles in the whole body, here I focused on the anti-inflammatory response in adipose tissue, because inflammation originating from excessive amount of visceral fat is considered as one of the main driving forces in the development of metabolic abnormality in obese individuals. CCL2, a potent chemotactic factor for monocyte, is produced predominantly by macrophages and its abundance in adipose tissue is increased in obese mice (Sartipy and Loskutoff 2003). In the adipose tissue, increased CCL2 signaling through its receptor, CCR2, links obesity and insulin

resistance through the induction of an inflammatory response (Kanda, Tateya et al. 2006). I found that macrophage-related genes, exemplified by *Ccl2*, *Adgre1*, and *Cd68* were upregulated in epididymal fat of HFD-fed DIO mice compared to normal mice, and chronic D5D-inhibition decreased the expression of these genes, thereby improvement on inflammation could be expected in the adipose tissue while further studies are necessary in order to clarify the association. I also confirmed a decrease in the AA to DGLA ratio in epididymal fat due to D5D-inhibition, and these changes could contribute toward improved insulin sensitivity by suppressing systemic inflammation in the adipose tissue. It is reported that insulin stimulates D5D and D6D gene expression in hepatocytes via a cAMP dependent mechanism (Rimoldi, Finarelli et al. 2001). Hence, increased D5D and D6D mRNA expression observed in fat tissue would be caused by improved insulin sensitivity. Leptin is a hormone synthesized and released by WAT, and plays an important role in maintaining energy balance and regulation of BW (Zhang, Proenca et al. 1994). In my results, chronic D5D-inhibition led to a marked decrease in leptin mRNA expression in epididymal fat, which could largely be attributed to body fat loss and improved leptin resistance.

Body fat accumulation, and consequently increase in BW, fluctuates in accordance with the difference between energy intake and EE over time. Here, I examined energy balance in detail and found that chronic D5D-inhibition significantly increased daily EE. The increase in EE with a concomitant slight decrease in energy intake resulted in a severe negative energy balance responsible for the observed fat and weight loss. Some interventions, which modulate metabolic fluxes in adipocytes, result in a general decrease in the accumulation of body fat. Pharmacological stimulation of PPARα (Hondares, Rosell et al. 2011) or leptin treatment (Wang, Lee et al. 1999) increase UCP1 positive cells in WAT, which mediate thermogenesis and mitochondrial uncoupling, and they are known as beige fat cells. It was reported that dietary AA has a negative influence on the production of beige fat cells upon β3-adrenergic receptor stimulation (Pisani, Ghandour et al. 2014). Therefore, I evaluated the expression levels

of beige fat cell-selective genes such as *Ucp1*, *Elovl3*, *Cid*ea, and *Otop*1 in subcutaneous fat, but no change was observed upon D5D-inhibition.

AA is also the substrate for the synthesis of anandamide and other endocannabinoids. It is well known that rimonabant, a selective inverse agonist of cannabinoid receptor 1 (CB1), has shown to cause weight loss due to decreased food intake and increased EE (Zhang, Gamo et al. 2012). Studies in rodents indicated that chronic rimonabant treatment upregulated UCP1 expression both in interscapular brown adipose tissue (BAT) and WAT adipocytes via increased sympathetic activity (Verty, Allen et al. 2009, Perwitz, Wenzel et al. 2010). Although D5D-inhibition showed much less impact on food reduction and UCP1 induction in WAT, decreased cannabinoid signaling in BAT may exert increased EE through a similar mechanism as chronic rimonabant treatment. Thus, while increased EE by chronic D5D-inhibition may contribute to its anti-obesity effect, further studies are required to delineate the mechanism of the increase in EE.

Contrary to these beneficial effects of D5D-inhibition, there are two major concerns for future development. One of the considerable concerns is the fact that D5D-inhibition also affects the n-3 PUFA desaturation pathway. Here, I observed decreased blood and tissue levels of DHA and EPA by D5D-inhibition in mice. Although any abnormal findings were not observed in the mice with pharmacological D5D-inhibition even in the absence of EPA and DHA intake (Table 2), this on-target effect may have some negative impact from the therapeutic point of view due to the increasing number of the positive evidence of n-3 PUFA on human health (Swanson, Block et al. 2012, Dyall 2015). Another possible concern is the risk of varying efficacy under the different PUFA composition in foods. In the current experiments, I used the HFD that contains high amount of LA and low or no amount of AA (Table 2), and exemplified the possibility that the D5D-inhibition may exert both anti-inflammatory and anti-obesity effects when taking the high-LA diet, such as western-style diets. On the other hand, dietary intake of AA or other PUFA may attenuate the therapeutic efficacy

of D5D-inhibition in line with the increase in blood and tissue AA/DGLA ratio. Therefore, more experiments are necessary to elucidate the mechanism of action of D5D-inhibition on anti-obesity and anti-inflammatory potentials, and clear mitigation plans for potential concerns and problems are required.

In conclusion, I showed the availability of the blood AA to DGLA ratio as a useful PD marker for D5D-inhibition. I also confirmed a sub-chronic effect of D5D-inhibition on insulin sensitivity and body fat loss with increased EE. Although further characterization is required to understand the physiological and pathophysiological impact on PUFA-desaturase pathways, D5D selective inhibition will be a new strategy for the improvement of obese and diabetic patients.

Chapter 2: GPR40 mediated signal contributes to pancreatic hormone secretion

Abstract

G protein-coupled receptor 40 (GPR40)/free fatty acid 1 (FFA1) is a G protein-coupled receptor involved in free fatty acid-induced insulin secretion. To analyze the effect of GPR40-selective activation on insulin and glucagon secretion, I performed hormone secretion assays and measured intracellular Ca^{2+} concentration ($[Ca^{2+}]_i$) using TAK-875, a synthetic GPR40 selective agonist, in both human and rat islets. Insulin and glucagon secretion were measured in static and dynamic conditions by using groups of isolated rat and human pancreatic islets. $[Ca^{2+}]_i$ was recorded by using confocal microscopy. GPR40 expression was measured by quantitative polymerase chain reaction. In both human and rat islets, stimulation of GPR40 signal enhanced glucose-stimulated insulin secretion in a glucose-dependent manner. The stimulatory effect by GPR40 agonist was similar to that produced by glucagon-like peptide-1 and correlated with the elevation of β-cell $[Ca^{2+}]_i$. Activation of GPR40 signal was without effect on glucagon secretion at both 1 and 16 mM glucose in human islets. These data indicate that GPR40 influences mainly insulin secretion in a glucose-dependent manner. The β-cell-specific action of GPR40 agonist in human islets may represent a therapeutically useful feature that allows plasma glucose control without compromising counter-regulation of glucagon secretion, thus minimizing the risk of hypoglycemia.

Introduction

Insulin and glucagon have opposite effects on the regulation of plasma glucose levels. Insulin, which is secreted from pancreatic β-cells in response to increased plasma glucose, decreases hepatic glucose production and increases glucose uptake in multiple tissues (Frayn 2003). Impaired insulin secretion is a major cause of the onset and development of type 2 diabetes, and drugs that enhance insulin secretion, such as sulfonylureas and glinides, are

commonly used for its treatment (Marchetti, Dotta et al. 2008). On the other hand, glucagon secretion from pancreatic α-cells is suppressed in response to elevated blood glucose levels, whereas reduced blood glucose enhances glucagon release. Glucagon is the principal hormone stimulating hepatic glucose production. Glucagon secretion is inappropriately high at elevated plasma glucose levels in diabetic patients, which contributes significantly to the hyperglycemia that is a hallmark of the disease (Shah, Basu et al. 1999). Thus, impaired regulation of both insulin and glucagon secretion plays a prominent role in the etiology of diabetes.

The mechanism of insulin secretion from β-cells is well understood: glucose metabolism increases the intracellular ATP/ADP ratio, which in turn closes ATP-sensitive potassium channels (K_{ATP} channels) and activates voltage-gated calcium channels (Ca^{2+} channels) (Fig. 17). The resultant stimulation of Ca^{2+} influx and associated elevation of $[Ca^{2+}]_i$ triggers insulin exocytosis (MacDonald, Joseph et al. 2005). The mechanisms regulating glucagon secretion from α-cells remain debated. It has been suggested that glucose can suppress glucagon secretion through a direct effect on α-cell activity (Gromada, Ma et al. 2004), but there is also evidence that glucagon secretion is under paracrine and neuronal control (Miki, Liss et al. 2001, Gromada, Franklin et al. 2007). Although the precise mechanism by which glucose regulates glucagon secretion is currently unclear, there is consensus that glucagon secretion from α-cells depends on an elevated $[Ca^{2+}]_i$ (Nadal, Quesada et al. 1999). Spontaneous $[Ca^{2+}]_i$ oscillations are seen in α-cells exposed to low glucose concentrations (i.e., conditions associated with the stimulation of glucagon release). Glucose-induced suppression of glucagon secretion has been proposed to involve a reduction of $[Ca^{2+}]_i$ (Berts, Gylfe et al. 1995, Quesada, Nadal et al. 1999, Barg, Galvanovskis et al. 2000, Gopel, Kanno et al. 2000), but there are conflicting data (Le Marchand and Piston 2010).

Free fatty acids (FFA) act as a primary energy source in the body, but they also act as systemic and intracellular signaling modulators. Acute exposure to FFA leads to the stimulation of insulin secretion (Olofsson, Salehi et al. 2004), whereas prolonged exposure leads to the

inhibition of glucose-stimulated insulin secretion (Olofsson, Collins et al. 2007, Hoppa, Collins et al. 2009). FFA also influence glucagon secretion from isolated mouse islets (Olofsson, Salehi et al. 2004). The acute effects involve stimulation of glucagon secretion at both high and low glucose concentrations, whereas long-term exposure is associated with stimulated release at low glucose levels and loss of glucose-induced suppression (Collins, Salehi et al. 2008). These effects of FFA on insulin and glucagon secretion require transport of the FFA across the plasma membrane and metabolism by long-chain FA-CoA (Prentki, Joly et al. 2002). However, the finding that FFA also act as a ligand of G protein-coupled receptor 40 (GPR40) suggests an alternative or additional regulatory mechanism (Morgan and Dhayal 2009). GPR40 was found as an orphan G protein-coupled receptor, and it couples mainly with Gαq protein (Itoh, Kawamata et al. 2003, Fujiwara, Maekawa et al. 2005, Tomita, Masuzaki et al. 2006) (Fig. 17). The activation of GPR40 by FFA increases $[Ca^{2+}]_i$ by a Gαq-mediated pathway and thus stimulates insulin secretion in a glucose-dependent manner (Fujiwara, Maekawa et al. 2005). In rodents, GPR40 is highly expressed in pancreatic β-cells, but the expression within α-cells remains controversial (Flodgren, Olde et al. 2007, Hirasawa, Itsubo et al. 2008). GPR40 is highly expressed in human pancreatic islets (Tomita, Masuzaki et al. 2006), but there is little information about the cellular distribution of GPR40 within an islet.

TAK-875 is a potent and highly selective agonist for GPR40 and improves glucose tolerance via stimulation of glucose-induced insulin secretion in type 2 diabetic rats (Negoro, Sasaki et al. 2010, Tsujihata, Ito et al. 2011). The possibility that GPR40 activation may possesse a glucose-dependent mode of action, thus minimizing the risk of hypoglycemia, makes it a promising candidate for future diabetes therapy. Here, I have compared the effects of GPR40 activation on insulin and glucagon secretion in isolated human and rat pancreatic islets. My data suggest that whereas GPR40 signal influences insulin and glucagon secretion in rat islets, its effect is restricted to insulin secretion in human islets.

Materials and Methods

Cell culture

Rat islets were isolated from pancreas of 180- 250-g female Sprague-Dawley rats by digestion with collagenase type-IV (Sigma) solution dissolved in HBSS (Sigma) at a final concentration of 1.9 U/mL. Islets were handpicked under a stereomicroscope and cultured overnight in RPMI1640 medium (GIBCO) containing 10% FCS, penicillin (100 U/mL), streptomycin (100 μg/mL), and 5 mM glucose at 37°C in 95% air with 5% CO_2. Human pancreases were obtained with ethical approval and clinical consent from non-diabetic donors. Islets were isolated by collagenase digestion in the Diabetes Research and Wellness Foundation Human Islet Isolation Facility (University of Oxford) using established methods (Ricordi, Lacy et al. 1988). Human islets were cultured in H-cell medium (SBMI 06, H-cell technology Inc., USA) at 37°C in 95% air with 5% CO_2.

Chemicals

TAK-875 (Negoro, Sasaki et al. 2010) was synthesized in the Chemical Development Laboratories at Takeda Pharmaceutical Company Limited, and dissolved in DMSO. Glucagon-like peptide-1 (7-37) amide (GLP-1) was purchased from Bachem (Weil am Rhein, Germany).

Static incubation assay

Krebs-Ringer bicarbonate HEPES buffer (KRBH) containing 130 mM NaCl, 5 mM KCl, 1 mM $MgSO_4$, 1 mM NaH_2PO_4, 27 mM $NaHCO_3$, 25 mM HEPES and 2.8 mM $CaCl_2$ supplemented with 0.2% FFA-free BSA (Sigma) was used as the assay buffer. After overnight culture, batches of 8-10 islets were washed twice with RPMI 1640 medium containing 10% FCS, penicillin (100 U/mL) and streptomycin (100 μg/mL) in assay tubes, and pre-incubated for 1 h with assay buffer containing 1 mM glucose at 37°C. The extracellular buffer was then

substituted with assay buffer (0.3 mL) containing 1 or 16 mM glucose with 0.1% DMSO (control) or test substances (dissolved in an equal amount of DMSO). After 1 h incubation at 37°C, aliquots for subsequent measurements of insulin and glucagon were taken. Insulin was measured with a rat insulin RIA kit (Linco, USA) or human insulin-specific RIA kit (Linco, USA). Secreted glucagon was measured with a glucagon RIA kit (Linco, USA). Islet insulin and glucagon contents were measured after acid ethanol (0.15 mL; 0.18 mM HCl, in 70% ethanol) extraction of islet homogenates.

Islet perifusion analysis

Time-dependent change in insulin release from isolated islets was assessed using a multi-chamber perifusion system maintained at 37°C. Batches of 160 islets were loaded into Millipore chambers (Swinnex 13; 1 μm filter) and pre-perifused (0.5 ml/min) for 30 min with KRBH at initial glucose concentration (5 mM) with 0.1% DMSO (control) or TAK-875 (3 μM). The perifusion buffers were then switched to the buffers containing different concentrations of glucose with 0.1% DMSO or TAK-875, and perifusate samples were collected every 1-2 min. Secreted insulin and islet insulin content (extracted by acid ethanol) were determined as described above.

Intracellular Ca^{2+} measurements

Intact rat or human islets were loaded with 2 μM fluo-4-AM (Molecular Probes) in RPMI 1640 (GIBCO) medium containing FFA-free BSA (0.01% for rat islets, and 0.2% for human islets), penicillin (100 U/mL), streptomycin (100 μg/mL) and 5 mM glucose for at least 2 h at room temperature before the imaging experiments commenced. Islets were immobilized with a wide-bore holding pipette in a continuously superfused and temperature-controlled (37°C) bath mounted on the stage of an Axioskop 2 FS-mot microscope (Carl Zeiss). KRBH supplemented with 0.01% FFA-free BSA was used as a perifusion buffer. Images were

collected using an LSM 510 system (Carl Zeiss) at 1.48-second intervals. Excitation was with a 488 nm argon laser, and emitted fluorescence was collected through 500-550 nm band-pass filters for the fluo-4 signal. Prior to experimental recordings, islets were perifused for 10 min with the perifusion buffer with 1 mM glucose and 0.1% DMSO. This was followed by perifusion with a buffer containing 16 mM glucose and 0.1% DMSO (v/v) and finally by 16 mM glucose plus 3 μM TAK-875 (in 0.1% DMSO). The $[Ca^{2+}]_i$ response was determined by baseline subtraction and plotted as change in fluorescence intensity (%ΔF/F), expressed as follows: $\%\Delta/F = (F_{(t)}-F_{min})/(F_{max}-F_{min})\times 100$. Single β- and α-cells within islets were identified by their reciprocal regulation by glucose as previously described (Berts, Gylfe et al. 1995, Quesada, Nadal et al. 1999, Barg, Galvanovskis et al. 2000, Gopel, Kanno et al. 2000). Briefly, when glucose concentration is switched from low (1 mM) to high (16 mM), insulin-secreting β-cells show transient spikes or sustained increase of $[Ca^{2+}]_i$. On the other hand, glucagon-secreting α-cells present $[Ca^{2+}]_i$ oscillations in response to low glucose tend to become silent at high glucose (MacDonald, De Marinis et al. 2007). To evaluate the effects of GPR40 activation, the area under the $[Ca^{2+}]_i$-curve for each given treatment period was calculated and reported as arbitrary units (AU).

Quantification of mRNA expression of GPR40 and other receptor genes

Four batches of human islets were used in these experiments. Total RNA was extracted from 50-100 human islets and purified using a QIA shredder and QIAGEN RNeasy Mini Kit (QIAGEN, Germany). Genome DNA was digested using RNase-free DNase (QIAGEN). First-strand cDNA was synthesized by random hexamer-primed reverse transcription using a TaqMan Reverse Transcription Reagents kit (Applied Biosystems, USA). The mRNA levels were quantified by an ABI Prism 7900 TaqMan PCR system (Applied Biosystems) according to manufacturer's instruction using TaqMan® Universal PCR Mastermix (Applied Biosystems). Copy numbers of the target genes were determined by the standard curve method using

synthesized and PAGE-purified oligo DNA fragments (Sigma Genesis, UK) containing the PCR amplicon regions. The mRNA expression in each gene was normalized to that of GAPDH. The specific primers and probes were synthesized (Applied Biosystems) according to published sequences (Tomita, Masuzaki et al. 2006). Primer sequences are given in table 4.

Statistical analysis

Results were expressed as mean ± *SEM*. Statistical analysis between two groups was assessed by Student's *t*-test or the Aspin-Welch test as indicated. A *p*-value of ≤ 0.05 was considered statistically significant. The dose-dependent effects of TAK-875 vs. control on hormone secretion assays were evaluated by the one-tailed Williams' test and a *p*-value of ≤ 0.025 was considered significant.

Results

GPR40 signal on insulin and glucagon secretion in isolated rat islets

In rat islets, high glucose (16 mM) increased insulin secretion 3.3-fold compared to low glucose (1 mM). Addition of TAK-875 (0.1-1 μM) or GLP-1 (0.01 μM) potentiated the stimulatory effect of high glucose but both compounds were ineffective at the low glucose concentration (Fig. 18A). As expected, increasing glucose from 1 to 16 mM resulted in reduced glucagon secretion. Consistent with what is observed in mouse islets (De Marinis, Salehi et al. 2010), GLP-1 inhibited glucagon secretion at low glucose and 0.1 μM TAK-875 was equally inhibitory. A 10-fold higher concentration of TAK-875 did not inhibit glucagon secretion in excess of the inhibition produced by 0.1 μM. Neither compound enhanced the inhibitory effect of high glucose (Fig. 18B).

GPR40 signal on 1st and 2nd phases of insulin secretion at high glucose in perifused rat islets

To analyze the effect of GPR40 activation on 1st and 2nd phase insulin secretion, dynamic measurements of insulin secretion were obtained by perifusion of isolated rat islets. As shown in Fig. 19A, TAK-875 (3 μM) had no stimulatory effect on insulin secretion at 5 or 1 mM glucose and, if anything, inhibited secretion. However, a strong stimulation was observed at 16 mM glucose. The stimulatory effect was particularly pronounced for 2nd phase insulin secretion; the area under the curve (AUC) measured during 1st (62-69 min) and 2nd phase (70-82 min) increased 2.3- and 3.9-fold, respectively (Fig. 19B). The stimulatory effect of 16 mM glucose in both the absence and presence of GPR40 agonist was promptly reversed upon reduction of glucose to 5 mM.

GPR40 signal on $[Ca^{2+}]_i$ in individual cells within intact rat islets

I next examined the effects of TAK-875 (3 μM) on $[Ca^{2+}]_i$ responses in individual β- and α-cells within isolated intact rat islets (Fig. 20A). When glucose concentration was switched from low (1 mM) to high (16 mM), β-cells responded with either transient spikes or a sustained increase in $[Ca^{2+}]_i$. Addition of GPR40 agonist at high glucose concentration resulted in a further elevation of $[Ca^{2+}]_i$ in β-cells (Fig. 20B; Rβ1, 2). In α-cells, identified by the generation of $[Ca^{2+}]_i$ oscillations at 1 mM glucose, increasing glucose to 16 mM reduced the amplitude of, but did not suppress, these $[Ca^{2+}]_i$ oscillations. These effects of glucose were not changed by the inclusion of GPR40 agonist in the superfusion medium (Fig. 20B; Rα1, 2). The effects of glucose and GPR40 agonist on β- and α-cell $[Ca^{2+}]_i$ are indicated in Fig. 20C and D.

Comparison of gene expression levels of GPR40, GLP-1R and SUR1 in human islets

GPR40 is highly expressed in rodent islets but there is little information about the expression levels in human islets. Therefore, I first quantified mRNA expression of *GPR40* in human islets from four non-diabetic organ donors. Donor characteristics are given in table 5. The expression of *GPR40* in human islets was comparable to that of the GLP-1 receptor (*GLP-1R*) (Fig. 21). Expression of *GPR40* was also compared to the K_{ATP}-channel subunit *SUR1*. Again, *GPR40* expression was found to be at least as high as that of the reference gene. Thus, *GPR40* is expressed in human islets at levels comparable to or higher than those of two other genes that encode proteins with key roles in islet/β-cell function. This prompted me to investigate the effects of GPR40 agonist on insulin and glucagon secretion from human islets.

GPR40 signal on insulin and glucagon secretion in isolated human islets

The effects of TAK-875 at 1 or 16 mM glucose on insulin and glucagon secretion in human islets were measured in static incubations. A total of 4 donors was used for the experiments reported here (Table 5). The responses observed with islets from individual donors are summarized in table 6. Fig. 22 presents the mean responses for all four donors. Since the amount of secreted insulin and glucagon varied among these four batches, they were expressed as % of each control (low glucose alone). It is evident that 16 mM glucose stimulates insulin secretion >3-fold and that this effect is enhanced by 3 µM TAK-875; lower concentrations tended to increase insulin secretion but this effect did not reach statistical significance. The effect of GPR40 activation was comparable to the stimulation observed in response to GLP-1; no stimulation by GPR40 activation was observed at 1 mM glucose. Increasing glucose to 16 mM glucose inhibited glucagon secretion. GPR40 activation was without effect on glucagon secretion at any of the concentrations tested at 1 or 16 mM glucose. GLP-1 did not exert an additive inhibitory effect when applied in the presence of 16 mM glucose (Fig. 22B).

GPR40 signal on $[Ca^{2+}]_i$ in individual cells within intact human islets

The effects of TAK-875 (3 μM) on $[Ca^{2+}]_i$ responses in individual β- and α-cells were also investigated in intact human islets from three non-diabetic donors (Fig. 23A). The donor characteristics are given in table 5. As observed in rat islets, human β-cells responded with elevation of $[Ca^{2+}]_i$ when glucose concentration was switched from 1 to 16 mM glucose, and the addition of GPR40 agonist to islets already exposed to high glucose resulted in a further elevation in many of the β-cells (Fig. 23B; Hβ 1-2). Fig. 23C summarizes the effects of 16 mM glucose in the absence and presence of GPR40 agonist. As in rat islets, I observed cells that were spontaneously active at 1 mM glucose and that are therefore likely to be α-cells. However, a spontaneous time-dependent decrease in the amplitude of these oscillations made it difficult to evaluate the effects of glucose and GPR40 agonist, and I therefore refrained from quantitative analysis of these data from α-cells.

Discussion

Because activation of GPR40 signaling evoked by medium- or long-chain FFA enhances glucose-stimulated insulin secretion (Itoh, Kawamata et al. 2003, Fujiwara, Maekawa et al. 2005), potent and specific GPR40 agonists may be useful for the treatment of T2DM Although published reports show that small-molecule agonists for GPR40 stimulate glucose-dependent insulin secretion in both *in vitro* and *in vivo* rodent models (Briscoe, Peat et al. 2006, Bharate, Nemmani et al. 2009), there is as yet no evidence that GPR40 agonists are effective in human islets. In addition, the effects of selective GPR40 agonists on glucagon secretion have not been elucidated. Here, I have examined the effects of GPR40 agonist, TAK-875, on insulin and glucagon secretion and $[Ca^{2+}]_i$ in rat and human pancreatic islets. The significance of such comparative studies is highlighted by electrophysiological studies demonstrating major

differences in the ion channel complements expressed in human and rodent islet cells (Braun, Ramracheya et al. 2008, Ramracheya, Ward et al. 2010). It is unlikely that these differences will be restricted to ion channels and those are already documented.

I found that GPR40 is expressed at levels comparable with those for GLP-1R and SUR1 in human islets. Similar results have been reported in rat islets (Itoh, Kawamata et al. 2003). GLP-1R and SUR1 play important roles in β-cell function, and they constitute to the molecular targets of two groups of insulinotropic drugs: GLP-1 analogs and sulfonylureas. I showed that GPR40 agonist augments glucose-stimulated insulin secretion in a way reminiscent of the action of GLP-1 in both rat and human islets. The dynamic measurements of insulin secretion reveal that although GPR40 agonist enhances both first- and second-phase insulin secretion in a strictly glucose-dependent fashion, the stimulatory effect is particularly pronounced for second-phase release.

The insulin-releasing capacity of GPR40 agonist correlated with elevation of $[Ca^{2+}]_i$. It has been proposed that GPR40, via inositol trisphosphate production, mobilizes Ca^{2+} from the endoplasmic reticulum (Fujiwara, Maekawa et al. 2005). Alternatively, GPR40 signal may act by enhancing entry of extracellular Ca^{2+} via the voltage-gated Ca^{2+} channels. This could result from a direct effect on the voltage-gated Ca^{2+} channels or an indirect effect caused by closure of the K_{ATP} channels (Feng, Luo et al. 2006). The exact mechanism of the glucose-dependent insulinotropic action of GPR40 signal remains to be elucidated and is beyond the scope of the current investigation, the primary objective of which was to compare the action of GPR40 stimulation on hormone secretion from human and rat islets.

The human islet preps showed some heterogeneity in insulin secretion, and one batch (donor 7) was unresponsive to 1 μM TAK-875 (Table 6), but it should be noted that the same islets responded to the agonist with an elevation of $[Ca^{2+}]_i$ (Fig. 24). Studies on islets from a greater number of donors are therefore needed to determine whether there is a true heterogeneity in responsiveness to GPR40 activation.

I also showed that GPR40 activation tends to inhibit rather than stimulate glucagon secretion induced by low glucose in rat islets, but without effect on glucagon secretion from human islets. The presence of GPR40 in rodent α-cells is debated (Flodgren, Olde et al. 2007, Hirasawa, Itsubo et al. 2008). However, GPR40 expression in human islets seems dominant in insulin-positive cells (Itoh, Kawamata et al. 2003, Tomita, Masuzaki et al. 2006). Thus, one explanation for the lack of glucagonostatic action in human islets might reflect the low GPR40 expression in human α-cells. Another explanation is that GPR40 activation might affect paracrine factors, such as somatostatin secretion, and the contribution might be different between species.

It was reported that linoleic acid, one of the endogenous agonists for GPR40, stimulates glucagon secretion in rodent islets (Flodgren, Olde et al. 2007, Wang, Zhao et al. 2011). By contrast, my results indicate that GPR40 agonist is without stimulatory effect on glucagon secretion in both rat and human islets and if anything tends to inhibit glucagon secretion in rat islets exposed to low glucose. TAK-875 is >400-fold more potent at activating human GPR40 than oleic acid, which shows agonist activity almost similar to that of linoleic acid (Tsujihata, Ito et al. 2011). These results clearly suggest that, unlike physiological agonists, the activation of GPR40 by a selective synthesized agonist has no potential to enhance glucagon secretion.

With regard to the interaction of TAK-875 with the endogenous ligands (FFA), it is of interest that TAK-875 potently stimulates insulin secretion during oral glucose tolerance tests in diabetic rats fasted overnight, in which plasma FFA levels are elevated because of the stimulation of lipolysis (Tsujihata, Ito et al. 2011). These data suggest that TAK-875 may show positive cooperativity with endogenous ligands. The role of GPR40 in FFA-regulated glucagon secretion merits further studies, and it deserves pointing out that FFA may influence glucagon secretion by mechanisms that do not involve GRP40 (Olofsson, Salehi et al. 2004).

As for the glucagonostatic action of GPR40 agonist at 1 mM glucose in rat islets, a lower dose (0.1 μM) is paradoxically more potent than a higher dose (1 μM). The underlying

mechanisms are unclear but it is worth remembering that this “anomaly” is shared with other modulators of glucagon secretion. Thus, glucose, adrenaline, and forskolin inhibit glucagon secretion at a low concentration, whereas higher concentrations are less inhibitory (glucose; (Vieira, Salehi et al. 2007)) or even stimulatory (adrenaline and forskolin; (De Marinis, Salehi et al. 2010)).

My data suggest that the effects of GPR40 agonist on glucagon secretion differ between rat and human islets. This underscores the importance of confirming in human islets observations made in rodent islets. The clinical relevance of the lack of effect of GPR40 agonist on glucagon secretion remains to be determined. Diabetes is associated with hypersecretion of glucagon at elevated plasma glucose levels. Pharmacological treatment of hyperglycemia and hypoinsulinemia is complicated by an impaired counter-regulation by glucagon during hypoglycemia. From this perspective, it may be argued that the selective action of GPR40 activation on insulin secretion at high glucose may be clinically beneficial.

General Discussion

Metabolic syndrome (MS) is a complex disorder defined by a cluster of interconnecting factors which lead to life-threatening comorbidities, and a concept of metabolic domino has been proposed to capture the flow of events and chain reactions. To clarify the contribution of fatty acids mediated signals on the onset of MS, I examined the physiological importance of delta-5-desaturase (D5D) mediated metabolism on the obesity and insulin resistance (Chapter 1), and G-protein coupled receptor 40 (GPR40) on the glucose-stimulated insulin secretion from the pancreatic islets (Chapter 2).

In the first chapter, I found the evidence that sub-chronic pharmacological inhibition of D5D improves insulin sensitivity and body fat loss with increased EE in DIO mice. My results were consistent with the fact that D5D KO mice shows beneficial metabolic phenotype for obesity, diabetes, and atherosclerotic cardiovascular disease (Powell, Gay et al. 2016). Although further characterization is required, my data suggest that induction of EE and anti-inflammatory action are potential mechanisms of D5D inhibition for obesity and insulin resistance.

Contrary to the beneficial effects of D5D inhibition, I also discussed 2 potential concerns regarding pharmacological inhibition. 1) Since D5D also contributes to the n-3 PUFA desaturation pathway, decreased blood and tissue levels of DHA and EPA were observed in D5D inhibitor-treated mice. This on-target effect may have negative impacts on the therapeutic point of view based on the beneficial evidence of n-3 PUFA on human health (Swanson, Block et al. 2012, Dyall 2015). 2) The risk of varying efficacy of D5D inhibitor under the different PUFA composition in foods. Here I used the HFD which contains high amount of LA and low or no amount of AA. But unlike in laboratory animals, human can choose a wide variety of foods and drinks, and the impact of dietary AA contents on the efficacy of D5D inhibition should be evaluated for further understanding of the therapeutic potential. Therefore, more experiments are necessary to elucidate the mechanism of action of D5D inhibition on anti-obesity and anti-inflammatory potentials, and clear mitigation plans for potential concerns and problems are required.

In the second chapter, I investigated the influence of GPR40 agonist on insulin and glucagon secretion using rat and human isolated islets. At that time, the evidence that GPR40 agonist potentiates glucose-stimulated insulin secretion in human islets provided me confidence to proceed into the clinical trial. Consistent with my results, TAK-875 (Fasiglifam) showed glucose lowering efficacy in a 12 weeks phase 2 randomized, double-blind placebo control trial (Negoro, Sasaki et al. 2010, Burant, Viswanathan et al. 2012); unfortunately, the phase 3 trial was terminated due to the concerns of liver safety issue (Kaku, Enya et al. 2015).

Natural substrates of GPR40 include saturated (C12-C16) and unsaturated (C18-C20) FFA, which act as full agonists of GPR40 to mediate glucose-stimulated insulin secretion from pancreatic β-cells and GLP-1 secretion from intestinal cells (Kotarsky, Nilsson et al. 2003, Flodgren, Olde et al. 2007). On the contrary, TAK-875 that I used here is now recognized as a partial agonist of GPR40 which binds to the different sites, and it is known that TAK-875 and FFA synergistically stimulate insulin secretion both *in vitro* and *in vivo*. (Yabuki, Komatsu et al. 2013). However, I have done all of experiments reported here under no FFA, and the addition of physiological concentration of FFA might better mimic the condition in human patients.

Here, I pointed out the fact that effect of GPR40 agonist on glucagon secretion was different between rat and human islets. Although animal tissues are readily available, they sometimes failed to predict the results in the clinical trials (Akhtar 2015). And my results underscore the importance of confirming the investigation in human tissues for the drug discovery.

In conclusion, fatty acids and their metabolites affect multiple pathways regulating and maintaining the physiological functions. And my researches reported here strongly suggested that basic research of the fatty acids-mediated signals on the onset of MS are worthy for the disease understanding and future drug discovery.

Acknowledgements

I am deeply grateful to Professors Kenji Miura, Tomoki Chiba, Hidekazu Kuwayama, and Kazuto Nakada, at University of Tsukuba for guiding my work and valuable discussions through my doctoral program.

I am very thankful to Drs. Suichi Takagahara, Yumiko Okano Tamura, Ikuo Miyahisa, Junji Matsui, Hideo Suzuki, Shota Ikeda, Yoshiyuki Tsujihata, Koji Takeuchi, Masakuni Noda, Nobuhiro Suzuki, Masami Suzuki, Ryo Ito, Shiro Takekawa, Hideaki Nagaya, Hiroyuki Odaka, and Masatoshi Hazama, at Takeda Pharmaceutical Company Limited for guiding and valuable discussions through my work.

I am also thankful to Drs. Paul R.V. Johnson, Fernand Abdulkader, Reshma Ramracheya, Quan Zhang, Matthais Braun, Anne Clark, David R. Matthews, and Patrik Rorsman, at Oxford Centre for Diabetes, Endocrinology, and Metabolism (OCDEM) for valuable discussions and helpful suggestions.

Finally, I would like to appreciate my family for supporting my life in University of Tsukuba.

References

Aguilar, D. and S. D. Solomon (2006). "ACE inhibitors and angiotensin receptor antagonists and the incidence of new-onset diabetes mellitus: an emerging theme." Drugs **66** (9): 1169-1177.

Akhtar, A. (2015). "The flaws and human harms of animal experimentation." Camb Q Healthc Ethics **24** (4): 407-419.

Astorg, P., S. Bertrais, F. Laporte, N. Arnault, C. Estaquio, P. Galan, A. Favier and S. Hercberg (2008). "Plasma n-6 and n-3 polyunsaturated fatty acids as biomarkers of their dietary intakes: a cross-sectional study within a cohort of middle-aged French men and women." Eur J Clin Nutr **62** (10): 1155-1161.

Barg, S., J. Galvanovskis, S. O. Gopel, P. Rorsman and L. Eliasson (2000). "Tight coupling between electrical activity and exocytosis in mouse glucagon-secreting alpha-cells." Diabetes **49** (9): 1500-1510.

Baugh, S. D., P. K. Pabba, J. Barbosa, E. Coulter, U. Desai, J. P. Gay, S. Gopinathan, Q. Han, R. Hari, S. D. Kimball, H. V. Nguyen, C. Y. Ni, D. R. Powell, A. Smith, K. M. Terranova, A. Wilson, X. C. Yu and V. K. Lombardo (2015). "Design, synthesis, and in vivo activity of novel inhibitors of delta-5 desaturase for the treatment of metabolic syndrome." Bioorg Med Chem Lett **25** (18): 3836-3839.

Berts, A., E. Gylfe and B. Hellman (1995). "Ca2+ oscillations in pancreatic islet cells secreting glucagon and somatostatin." Biochem Biophys Res Commun **208** (2): 644-649.

Bharate, S. B., K. V. Nemmani and R. A. Vishwakarma (2009). "Progress in the discovery and development of small-molecule modulators of G-protein-coupled receptor 40 (GPR40/FFA1/FFAR1): an emerging target for type 2 diabetes." Expert Opin Ther Pat **19** (2): 237-264.

Bligh, E. G. and W. J. Dyer (1959). "A rapid method for total lipid extraction and purification." Patent WO2008089310A2 Can.J.Biochem.Physiol.(37): 911-917.

Braun, M., R. Ramracheya, M. Bengtsson, Q. Zhang, J. Karanauskaite, C. Partridge, P. R. Johnson and P. Rorsman (2008). "Voltage-gated ion channels in human pancreatic beta-cells: electrophysiological characterization and role in insulin secretion." Diabetes **57** (6): 1618-1628.

Briscoe, C. P., A. J. Peat, S. C. McKeown, D. F. Corbett, A. S. Goetz, T. R. Littleton, D. C. McCoy, T. P. Kenakin, J. L. Andrews, C. Ammala, J. A. Fornwald, D. M. Ignar and S. Jenkinson (2006). "Pharmacological regulation of insulin secretion in MIN6 cells through the fatty acid receptor GPR40: identification of agonist and antagonist small molecules." Br J Pharmacol **148** (5): 619-628.

Burant, C. F., P. Viswanathan, J. Marcinak, C. Cao, M. Vakilynejad, B. Xie and E. Leifke (2012). "TAK-875 versus placebo or glimepiride in type 2 diabetes mellitus: a phase 2, randomised, double-blind, placebo-controlled trial." Lancet **379** (9824): 1403-1411.

Chopra, M., S. Galbraith and I. Darnton-Hill (2002). "A global response to a global problem: the epidemic of overnutrition." Bull World Health Organ **80** (12): 952-958.

Collins, S. C., A. Salehi, L. Eliasson, C. S. Olofsson and P. Rorsman (2008). "Long-term exposure of mouse pancreatic islets to oleate or palmitate results in reduced glucose-induced somatostatin and oversecretion of glucagon." Diabetologia **51** (9): 1689-1693.

Covington, M. B. (2004). "Omega-3 fatty acids." Am Fam Physician **70** (1): 133-140.

De Marinis, Y. Z., A. Salehi, C. E. Ward, Q. Zhang, F. Abdulkader, M. Bengtsson, O. Braha, M. Braun, R. Ramracheya, S. Amisten, A. M. Habib, Y. Moritoh, E. Zhang, F. Reimann, A. Rosengren, T. Shibasaki, F. Gribble, E. Renstrom, S. Seino, L. Eliasson and P. Rorsman (2010). "GLP-1 inhibits and adrenaline stimulates glucagon release by differential modulation of N- and L-type Ca2+ channel-dependent exocytosis." Cell Metab **11** (6): 543-553.

De Marinis, Y. Z., A. Salehi, C. E. Ward, Q. Zhang, F. Abdulkader, M. Bengtsson, O. Braha, M. Braun, R. Ramracheya, S. Amisten, A. M. Habib, Y. Moritoh, E. Zhang, F. Reimann,

A. H. Rosengren, T. Shibasaki, F. Gribble, E. Renstrom, S. Seino, L. Eliasson and P. Rorsman (2010). "GLP-1 inhibits and adrenaline stimulates glucagon release by differential modulation of N- and L-type Ca2+ channel-dependent exocytosis." Cell Metab **11** (6): 543-553.

Dobbins, R. L., M. W. Chester, M. B. Daniels, J. D. McGarry and D. T. Stein (1998). "Circulating fatty acids are essential for efficient glucose-stimulated insulin secretion after prolonged fasting in humans." Diabetes **47** (10): 1613-1618.

Domei, T., H. Yokoi, S. Kuramitsu, Y. Soga, T. Arita, K. Ando, S. Shirai, K. Kondo, K. Sakai, M. Goya, M. Iwabuchi, M. Ueeda and M. Nobuyoshi (2012). "Ratio of serum n-3 to n-6 polyunsaturated fatty acids and the incidence of major adverse cardiac events in patients undergoing percutaneous coronary intervention." Circ J **76** (2): 423-429.

Dyall, S. C. (2015). "Long-chain omega-3 fatty acids and the brain: a review of the independent and shared effects of EPA, DPA and DHA." Front Aging Neurosci **7**: 52.

Erdmann, E., S. Harding, H. Lam and A. Perez (2016). "Ten-year observational follow-up of PROactive: a randomized cardiovascular outcomes trial evaluating pioglitazone in type 2 diabetes." Diabetes Obes Metab **18** (3): 266-273.

Feng, D. D., Z. Luo, S. G. Roh, M. Hernandez, N. Tawadros, D. J. Keating and C. Chen (2006). "Reduction in voltage-gated K+ currents in primary cultured rat pancreatic beta-cells by linoleic acids." Endocrinology **147** (2): 674-682.

Flodgren, E., B. Olde, S. Meidute-Abaraviciene, M. S. Winzell, B. Ahren and A. Salehi (2007). "GPR40 is expressed in glucagon producing cells and affects glucagon secretion." Biochem Biophys Res Commun **354** (1): 240-245.

Frayn, K. N. (2003). "Metabolic Regulation: A Human Perspective " Oxford Blackwell Science, Oxford, UK.

Fujiwara, K., F. Maekawa and T. Yada (2005). "Oleic acid interacts with GPR40 to induce Ca2+ signaling in rat islet beta-cells: mediation by PLC and L-type Ca2+ channel and link to insulin release." Am J Physiol Endocrinol Metab **289** (4): E670-677.

Glaser, C., J. Heinrich and B. Koletzko (2010). "Role of FADS1 and FADS2 polymorphisms in polyunsaturated fatty acid metabolism." Metabolism **59** (7): 993-999.

Gopel, S. O., T. Kanno, S. Barg, X. G. Weng, J. Gromada and P. Rorsman (2000). "Regulation of glucagon release in mouse -cells by KATP channels and inactivation of TTX-sensitive Na+ channels." J Physiol **528** (Pt 3): 509-520.

Gromada, J., I. Franklin and C. B. Wollheim (2007). "Alpha-cells of the endocrine pancreas: 35 years of research but the enigma remains." Endocr Rev **28** (1): 84-116.

Gromada, J., X. Ma, M. Hoy, K. Bokvist, A. Salehi, P. O. Berggren and P. Rorsman (2004). "ATP-sensitive K+ channel-dependent regulation of glucagon release and electrical activity by glucose in wild-type and SUR1-/- mouse alpha-cells." Diabetes **53 Suppl 3**: S181-189.

Haidar, Y. M. and B. C. Cosman (2011). "Obesity epidemiology." Clin Colon Rectal Surg **24** (4): 205-210.

Hirasawa, A., C. Itsubo, K. Sadakane, T. Hara, S. Shinagawa, H. Koga, H. Nose, T. A. Koshimizu and G. Tsujimoto (2008). "Production and characterization of a monoclonal antibody against GPR40 (FFAR1; free fatty acid receptor 1)." Biochem Biophys Res Commun **365** (1): 22-28.

Hondares, E., M. Rosell, J. Diaz-Delfin, Y. Olmos, M. Monsalve, R. Iglesias, F. Villarroya and M. Giralt (2011). "Peroxisome proliferator-activated receptor alpha (PPARalpha) induces PPARgamma coactivator 1alpha (PGC-1alpha) gene expression and contributes to thermogenic activation of brown fat: involvement of PRDM16." J Biol Chem **286** (50): 43112-43122.

Hoppa, M. B., S. Collins, R. Ramracheya, L. Hodson, S. Amisten, Q. Zhang, P. Johnson, F. M. Ashcroft and P. Rorsman (2009). "Chronic palmitate exposure inhibits insulin secretion by dissociation of Ca(2+) channels from secretory granules." Cell Metab **10** (6): 455-465.

Hornblad, A., A. Cheddad and U. Ahlgren (2011). "An improved protocol for optical projection tomography imaging reveals lobular heterogeneities in pancreatic islet and beta-cell mass distribution." Islets **3** (4): 204-208.

Inoue, K., K. Kishida, A. Hirata, T. Funahashi and I. Shimomura (2013). "Low serum eicosapentaenoic acid / arachidonic acid ratio in male subjects with visceral obesity." Nutr Metab (Lond) **10** (1): 25.

Itoh, H. (2006). "Metabolic domino: new concept in lifestyle medicine." Drugs Today (Barc) **42** Suppl C: 9-16.

Itoh, Y., Y. Kawamata, M. Harada, M. Kobayashi, R. Fujii, S. Fukusumi, K. Ogi, M. Hosoya, Y. Tanaka, H. Uejima, H. Tanaka, M. Maruyama, R. Satoh, S. Okubo, H. Kizawa, H. Komatsu, F. Matsumura, Y. Noguchi, T. Shinohara, S. Hinuma, Y. Fujisawa and M. Fujino (2003). "Free fatty acids regulate insulin secretion from pancreatic beta cells through GPR40." Nature **422** (6928): 173-176.

Kaku, K., K. Enya, R. Nakaya, T. Ohira and R. Matsuno (2015). "Efficacy and safety of fasiglifam (TAK-875), a G protein-coupled receptor 40 agonist, in Japanese patients with type 2 diabetes inadequately controlled by diet and exercise: a randomized, double-blind, placebo-controlled, phase III trial." Diabetes Obes Metab **17** (7): 675-681.

Kanda, H., S. Tateya, Y. Tamori, K. Kotani, K. Hiasa, R. Kitazawa, S. Kitazawa, H. Miyachi, S. Maeda, K. Egashira and M. Kasuga (2006). "MCP-1 contributes to macrophage infiltration into adipose tissue, insulin resistance, and hepatic steatosis in obesity." J Clin Invest **116** (6): 1494-1505.

Kirtland, S. J. (1988). "Prostaglandin E1: a review." Prostaglandins Leukot Essent Fatty Acids **32** (3): 165-174.

Knapp, H. R., O. Oelz, A. R. Whorton and J. A. Oates (1978). "Effects of feeding ethyl-dihomo-gamma-linolenate on rabbit renomedullary lipid composition and prostaglandin production in vitro." Lipids **13** (11): 804-808.

Kotarsky, K., N. E. Nilsson, E. Flodgren, C. Owman and B. Olde (2003). "A human cell surface receptor activated by free fatty acids and thiazolidinedione drugs." Biochem Biophys Res Commun **301** (2): 406-410.

Kremmyda, L. S., E. Tvrzicka, B. Stankova and A. Zak (2011). "Fatty acids as biocompounds: their role in human metabolism, health and disease: a review. part 2: fatty acid physiological roles and applications in human health and disease." Biomed Pap Med Fac Univ Palacky Olomouc Czech Repub **155** (3): 195-218.

Kroger, J., V. Zietemann, C. Enzenbach, C. Weikert, E. H. Jansen, F. Doring, H. G. Joost, H. Boeing and M. B. Schulze (2011). "Erythrocyte membrane phospholipid fatty acids, desaturase activity, and dietary fatty acids in relation to risk of type 2 diabetes in the European Prospective Investigation into Cancer and Nutrition (EPIC)-Potsdam Study." Am J Clin Nutr **93** (1): 127-142.

Le Marchand, S. J. and D. W. Piston (2010). "Glucose suppression of glucagon secretion: metabolic and calcium responses from alpha-cells in intact mouse pancreatic islets." J Biol Chem **285** (19): 14389-14398.

Lopez-Vicario, C., A. Gonzalez-Periz, B. Rius, E. Moran-Salvador, V. Garcia-Alonso, J. J. Lozano, R. Bataller, M. Cofan, J. X. Kang, V. Arroyo, J. Claria and E. Titos (2014). "Molecular interplay between Delta5/Delta6 desaturases and long-chain fatty acids in the pathogenesis of non-alcoholic steatohepatitis." Gut **63** (2): 344-355.

MacDonald, P. E., Y. Z. De Marinis, R. Ramracheya, A. Salehi, X. Ma, P. R. Johnson, R. Cox, L. Eliasson and P. Rorsman (2007). "A K ATP channel-dependent pathway within

alpha cells regulates glucagon release from both rodent and human islets of Langerhans." PLoS Biol **5** (6): e143.

MacDonald, P. E., J. W. Joseph and P. Rorsman (2005). "Glucose-sensing mechanisms in pancreatic beta-cells." Philos Trans R Soc Lond B Biol Sci **360** (1464): 2211-2225.

Marchetti, P., F. Dotta, D. Lauro and F. Purrello (2008). "An overview of pancreatic beta-cell defects in human type 2 diabetes: implications for treatment." Regul Pept **146** (1-3): 4-11.

Matthews, D. R., J. P. Hosker, A. S. Rudenski, B. A. Naylor, D. F. Treacher and R. C. Turner (1985). "Homeostasis model assessment: insulin resistance and beta-cell function from fasting plasma glucose and insulin concentrations in man." Diabetologia **28** (7): 412-419.

Mendis, S., L. H. Lindholm, G. Mancia, J. Whitworth, M. Alderman, S. Lim and T. Heagerty (2007). "World Health Organization (WHO) and International Society of Hypertension (ISH) risk prediction charts: assessment of cardiovascular risk for prevention and control of cardiovascular disease in low and middle-income countries." J Hypertens **25** (8): 1578-1582.

Miki, T., B. Liss, K. Minami, T. Shiuchi, A. Saraya, Y. Kashima, M. Horiuchi, F. Ashcroft, Y. Minokoshi, J. Roeper and S. Seino (2001). "ATP-sensitive K+ channels in the hypothalamus are essential for the maintenance of glucose homeostasis." Nat Neurosci **4** (5): 507-512.

Miyahisa, I., H. Suzuki, A. Mizukami, Y. Tanaka, M. Ono, M. S. Hixon and J. Matsui (2016). "T-3364366 Targets the Desaturase Domain of Delta-5 Desaturase with Nanomolar Potency and a Multihour Residence Time." ACS Med Chem Lett **7**(9): 868-872.

Monteiro, C. A., E. C. Moura, W. L. Conde and B. M. Popkin (2004). "Socioeconomic status and obesity in adult populations of developing countries: a review." Bull World Health Organ **82** (12): 940-946.

Morgan, N. G. and S. Dhayal (2009). "G-protein coupled receptors mediating long chain fatty acid signalling in the pancreatic beta-cell." Biochem Pharmacol **78** (12): 1419-1427.

Nadal, A., I. Quesada and B. Soria (1999). "Homologous and heterologous asynchronicity between identified alpha-, beta- and delta-cells within intact islets of Langerhans in the mouse." J Physiol **517** (Pt 1): 85-93.

Negoro, N., S. Sasaki, S. Mikami, M. Ito, M. Suzuki, Y. Tsujihata, R. Ito, A. Harada, K. Takeuchi, N. Suzuki, J. Miyazaki, T. Santou, T. Odani, N. Kanzaki, M. Funami, T. Tanaka, A. Kogame, S. Matsunaga, T. Yasuma and Y. Momose (2010). "Discovery of TAK-875: A Potent, Selective, and Orally Bioavailable GPR40 Agonist." ACS Med Chem Lett **1** (6): 290-294.

Negoro, N., S. Sasaki, S. Mikami, M. Ito, M. Suzuki, Y. Tsujihata, R. Ito, K. Takeuchi, N. Suzuki, J. Miyazaki, T. Santou, T. Odani, N. Kanzaki, M. Funami, T. Tanaka, A. Kogame, S. Matsunaga, T. Yasuma and Y. Momose (2010). "Discovery of TAK-875: A Potent, Selective, and Orally Bioavailable GPR40 Agonist." ACS Med. Chem, Lett. **1** (6): 290-294.

Ntambi, J. M., M. Miyazaki, J. P. Stoehr, H. Lan, C. M. Kendziorski, B. S. Yandell, Y. Song, P. Cohen, J. M. Friedman and A. D. Attie (2002). "Loss of stearoyl-CoA desaturase-1 function protects mice against adiposity." Proc Natl Acad Sci U S A **99** (17): 11482-11486.

Olofsson, C. S., S. Collins, M. Bengtsson, L. Eliasson, A. Salehi, K. Shimomura, A. Tarasov, C. Holm, F. Ashcroft and P. Rorsman (2007). "Long-term exposure to glucose and lipids inhibits glucose-induced insulin secretion downstream of granule fusion with plasma membrane." Diabetes **56** (7): 1888-1897.

Olofsson, C. S., A. Salehi, S. O. Gopel, C. Holm and P. Rorsman (2004). "Palmitate stimulation of glucagon secretion in mouse pancreatic alpha-cells results from activation of L-type calcium channels and elevation of cytoplasmic calcium." Diabetes **53** (11): 2836-2843.

Pan, A., V. S. Malik and F. B. Hu (2012). "Exporting diabetes mellitus to Asia: the impact of Western-style fast food." Circulation **126** (2): 163-165.

Park, H., G. Hasegawa, T. Shima, M. Fukui, N. Nakamura, K. Yamaguchi, H. Mitsuyoshi, M. Minami, K. Yasui, Y. Itoh, T. Yoshikawa, J. Kitawaki, M. Ohta, H. Obayashi and T. Okanoue (2010). "The fatty acid composition of plasma cholesteryl esters and estimated desaturase activities in patients with nonalcoholic fatty liver disease and the effect of long-term ezetimibe therapy on these levels." Clin Chim Acta **411** (21-22): 1735-1740.

Perwitz, N., J. Wenzel, I. Wagner, J. Buning, M. Drenckhan, K. Zarse, M. Ristow, W. Lilienthal, H. Lehnert and J. Klein (2010). "Cannabinoid type 1 receptor blockade induces transdifferentiation towards a brown fat phenotype in white adipocytes." Diabetes Obes Metab **12** (2): 158-166.

Pisani, D. F., R. A. Ghandour, G. E. Beranger, P. Le Faouder, J. C. Chambard, M. Giroud, A. Vegiopoulos, M. Djedaini, J. Bertrand-Michel, M. Tauc, S. Herzig, D. Langin, G. Ailhaud, C. Duranton and E. Z. Amri (2014). "The omega6-fatty acid, arachidonic acid, regulates the conversion of white to brite adipocyte through a prostaglandin/calcium mediated pathway." Mol Metab **3** (9): 834-847.

Powell, D. R., J. P. Gay, M. Smith, N. Wilganowski, A. Harris, A. Holland, M. Reyes, L. Kirkham, L. L. Kirkpatrick, B. Zambrowicz, G. Hansen, K. A. Platt, I. van Sligtenhorst, Z. M. Ding and U. Desai (2016). "Fatty acid desaturase 1 knockout mice are lean with improved glycemic control and decreased development of atheromatous plaque." Diabetes Metab Syndr Obes **9**: 185-199.

Prentki, M., E. Joly, W. El-Assaad and R. Roduit (2002). "Malonyl-CoA signaling, lipid partitioning, and glucolipotoxicity: role in beta-cell adaptation and failure in the etiology of diabetes." Diabetes **51** Suppl 3: S405-413.

Prentki, M., S. Vischer, M. C. Glennon, R. Regazzi, J. T. Deeney and B. E. Corkey (1992). "Malonyl-CoA and long chain acyl-CoA esters as metabolic coupling factors in nutrient-induced insulin secretion." J Biol Chem **267** (9): 5802-5810.

Proschak, E., P. Heitel, L. Kalinowsky and D. Merk (2017). "Opportunities and Challenges for Fatty Acid Mimetics in Drug Discovery." J Med Chem **60** (13): 5235-5266.

Quesada, I., A. Nadal and B. Soria (1999). "Different effects of tolbutamide and diazoxide in alpha, beta-, and delta-cells within intact islets of Langerhans." Diabetes **48** (12): 2390-2397.

Ramracheya, R., C. Ward, M. Shigeto, J. N. Walker, S. Amisten, Q. Zhang, P. R. Johnson, P. Rorsman and M. Braun (2010). "Membrane potential-dependent inactivation of voltage-gated ion channels in alpha-cells inhibits glucagon secretion from human islets." Diabetes **59** (9): 2198-2208.

Ricordi, C., P. E. Lacy, E. H. Finke, B. J. Olack and D. W. Scharp (1988). "Automated method for isolation of human pancreatic islets." Diabetes **37** (4): 413-420.

Rimoldi, O. J., G. S. Finarelli and R. R. Brenner (2001). "Effects of diabetes and insulin on hepatic delta6 desaturase gene expression." Biochem Biophys Res Commun **283** (2): 323-326.

Robertson, R. P., J. Harmon, P. O. Tran and V. Poitout (2004). "Beta-cell glucose toxicity, lipotoxicity, and chronic oxidative stress in type 2 diabetes." Diabetes **53** Suppl 1: S119-124.

Russo, C., O. Olivieri, D. Girelli, P. Guarini, R. Pasqualini, M. Azzini and R. Corrocher (1997). "Increased membrane ratios of metabolite to precursor fatty acid in essential hypertension." Hypertension **29** (4): 1058-1063.

Saito, E., T. Okada, Y. Abe, M. Odaka, Y. Kuromori, F. Iwata, M. Hara, H. Mugishima and Y. Kitamura (2013). "Abdominal adiposity is associated with fatty acid desaturase

activity in boys: implications for C-reactive protein and insulin resistance." Prostaglandins Leukot Essent Fatty Acids **88** (4): 307-311.

Sartipy, P. and D. J. Loskutoff (2003). "Monocyte chemoattractant protein 1 in obesity and insulin resistance." Proc Natl Acad Sci U S A **100** (12): 7265-7270.

Schonfeld, P. and L. Wojtczak (2016). "Short- and medium-chain fatty acids in energy metabolism: the cellular perspective." J Lipid Res **57** (6): 943-954.

Shah, P., A. Basu, R. Basu and R. Rizza (1999). "Impact of lack of suppression of glucagon on glucose tolerance in humans." Am J Physiol **277** (2 Pt 1): E283-290.

Simopoulos, A. P. (2002). "The importance of the ratio of omega-6/omega-3 essential fatty acids." Biomed Pharmacother **56** (8): 365-379.

Simopoulos, A. P. (2003). "Importance of the ratio of omega-6/omega-3 essential fatty acids: evolutionary aspects." World Rev Nutr Diet **92**: 1-22.

Speakman, J. R. (2013). "Measuring energy metabolism in the mouse - theoretical, practical, and analytical considerations." Front Physiol **4**: 34.

Steffen, L. M., B. Vessby, D. R. Jacobs, Jr., J. Steinberger, A. Moran, C. P. Hong and A. R. Sinaiko (2008). "Serum phospholipid and cholesteryl ester fatty acids and estimated desaturase activities are related to overweight and cardiovascular risk factors in adolescents." Int J Obes (Lond) **32** (8): 1297-1304.

Stein, D. T., V. Esser, B. E. Stevenson, K. E. Lane, J. H. Whiteside, M. B. Daniels, S. Chen and J. D. McGarry (1996). "Essentiality of circulating fatty acids for glucose-stimulated insulin secretion in the fasted rat." J Clin Invest **97** (12): 2728-2735.

Stoffel, W., I. Hammels, B. Jenke, E. Binczek, I. Schmidt-Soltau, S. Brodesser, M. Odenthal and M. Thevis (2014). "Obesity resistance and deregulation of lipogenesis in Delta6-fatty acid desaturase (FADS2) deficiency." EMBO Rep **15** (1): 110-120.

Suzuki, H., T. Fujimoto and T. Yamamoto Patent WO2010087467 A1.

Swanson, D., R. Block and S. A. Mousa (2012). "Omega-3 fatty acids EPA and DHA: health benefits throughout life." Adv Nutr **3** (1): 1-7.

Tomita, T., H. Masuzaki, H. Iwakura, J. Fujikura, M. Noguchi, T. Tanaka, K. Ebihara, J. Kawamura, I. Komoto, Y. Kawaguchi, K. Fujimoto, R. Doi, Y. Shimada, K. Hosoda, M. Imamura and K. Nakao (2006). "Expression of the gene for a membrane-bound fatty acid receptor in the pancreas and islet cell tumours in humans: evidence for GPR40 expression in pancreatic beta cells and implications for insulin secretion." Diabetologia **49** (5): 962-968.

Tschop, M. H., J. R. Speakman, J. R. Arch, J. Auwerx, J. C. Bruning, L. Chan, R. H. Eckel, R. V. Farese, Jr., J. E. Galgani, C. Hambly, M. A. Herman, T. L. Horvath, B. B. Kahn, S. C. Kozma, E. Maratos-Flier, T. D. Muller, H. Munzberg, P. T. Pfluger, L. Plum, M. L. Reitman, K. Rahmouni, G. I. Shulman, G. Thomas, C. R. Kahn and E. Ravussin (2012). "A guide to analysis of mouse energy metabolism." Nat Methods **9** (1): 57-63.

Tsujihata, Y., R. Ito, M. Suzuki, A. Harada, N. Negoro, T. Yasuma, Y. Momose and K. Takeuchi (2011). "TAK-875, an orally available G protein-coupled receptor 40/free fatty acid receptor 1 agonist, enhances glucose-dependent insulin secretion and improves both postprandial and fasting hyperglycemia in type 2 diabetic rats." J Pharmacol Exp Ther **339** (1): 228-237.

Verty, A. N., A. M. Allen and B. J. Oldfield (2009). "The effects of rimonabant on brown adipose tissue in rat: implications for energy expenditure." Obesity (Silver Spring) **17** (2): 254-261.

Vessby, B. (2003). "Dietary fat, fatty acid composition in plasma and the metabolic syndrome." Curr Opin Lipidol **14** (1): 15-19.

Vessby, B., I. B. Gustafsson, S. Tengblad, M. Boberg and A. Andersson (2002). "Desaturation and elongation of Fatty acids and insulin action." Ann N Y Acad Sci **967**: 183-195.

Vieira, E., A. Salehi and E. Gylfe (2007). "Glucose inhibits glucagon secretion by a direct effect on mouse pancreatic alpha cells." Diabetologia **50** (2): 370-379.

Wang, L., Y. Zhao, B. Gui, R. Fu, F. Ma, J. Yu, P. Qu, L. Dong and C. Chen (2011). "Acute stimulation of glucagon secretion by linoleic acid results from GPR40 activation and [Ca2+]i increase in pancreatic islet {alpha}-cells." J Endocrinol **210** (2): 173-179.

Wang, M. Y., Y. Lee and R. H. Unger (1999). "Novel form of lipolysis induced by leptin." J Biol Chem **274** (25): 17541-17544.

Warensjo, E., M. Ohrvall and B. Vessby (2006). "Fatty acid composition and estimated desaturase activities are associated with obesity and lifestyle variables in men and women." Nutr Metab Cardiovasc Dis **16** (2): 128-136.

Warensjo, E., M. Rosell, M. L. Hellenius, B. Vessby, U. De Faire and U. Riserus (2009). "Associations between estimated fatty acid desaturase activities in serum lipids and adipose tissue in humans: links to obesity and insulin resistance." Lipids Health Dis **8**: 37.

Wong, J. M., R. de Souza, C. W. Kendall, A. Emam and D. J. Jenkins (2006). "Colonic health: fermentation and short chain fatty acids." J Clin Gastroenterol **40** (3): 235-243.

Yabuki, C., H. Komatsu, Y. Tsujihata, R. Maeda, R. Ito, K. Matsuda-Nagasumi, K. Sakuma, K. Miyawaki, N. Kikuchi, K. Takeuchi, Y. Habata and M. Mori (2013). "A novel antidiabetic drug, fasiglifam/TAK-875, acts as an ago-allosteric modulator of FFAR1." PLoS One **8** (10): e76280.

Yaney, G. C. and B. E. Corkey (2003). "Fatty acid metabolism and insulin secretion in pancreatic beta cells." Diabetologia **46** (10): 1297-1312.

Zhang, L. N., Y. Gamo, R. Sinclair, S. E. Mitchell, D. G. Morgan, J. C. Clapham and J. R. Speakman (2012). "Effects of chronic oral rimonabant administration on energy budgets of diet-induced obese C57BL/6 mice." Obesity (Silver Spring) **20** (5): 954-962.

Zhang, Y., R. Proenca, M. Maffei, M. Barone, L. Leopold and J. M. Friedman (1994). "Positional cloning of the mouse obese gene and its human homologue." Nature **372** (6505): 425-432.

Zurier, R. B. (1991). "Role of prostaglandins E in inflammation and immune responses." Adv Prostaglandin Thromboxane Leukot Res **21B**: 947-953.

Tables

Table 1. Fatty acids mimetics proceeded into clinical trials

	Target	Endogenous ligands /substrates	Efficacy / Role	Mimetics that reached clinical use / trials
Nuclear receptor	PPARα	Eicosanoids, unsaturated fatty acids	energy homeostasis, fatty acids catabolism	Fibrates, Saroglitazar, Elafibranor
	PPARγ		glucose homeostasis, insulin sensitivity, anti-inflammatory	Glitazones, Saroglitazar, Elafibranor
	PPARδ		energy homeostasis, thermogenesis, proliferation, tissue repair	Elafibranor
	RXRs	Unknown	proliferation, differentiation, apoptosis	Alitretinoin, Bexarotene
	RARs	All-trans-retinoic acid, retinoids	growth/development, proliferation, differentiation, apoptosis, inflammation	Tazarotene, Adapalene
	FXR	Bile acids (CDCA)	bile acid homeostasis, lipid / glucose metabolism, liver inflammation	Obeticholic acid
Enzymes binding and metabolizing fatty acids	SCD1	Stearyl-CoA, Palmitoyl-CoA	endogenous synthesis of unsaturated fatty acids (oleyl-CoA, palmitoleyl-CoA)	Aramchol
	COX-1 COX-2	Arachidonic acid	cyclooxygenase pathway; formation of mediators of inflammation and pain, regulation of vascular tone and thrombocyte aggregation	NSADs NSAIDs, Coxibs
	5-LO	Arachidonic acid, 15(S)-HETE	lipoxygenase pathway; mediators of chemotaxis (LTA4, LXA_4), pulmonary inflammation, allergy, bronchoconstriction	Zileuton, Minocycline, Hyperforin
GPCR	FFAR1 (GP40)	Mediucm- and long-chain fatty acids (C6-C22)	incretin release, glucose-stimulated insulin secretion, tasting, inflammation	Fasiglifam (TAK-875)
	PGD_2 receptors (D_1 and D_2)	PGD_2	inflammation, pain, allergy	Laropiprant, Vidupiprant
	PGE_2 receptors (EP_{1-4})	PGE_2	inflammation, pain	Misoprostol
	$PGF_{2\alpha}$ receptors (FPA and FPB)	$PGF_{2\alpha}$		Latanoprost
	PGI_2 receptors (IP)	PGI_2 (prostacyclin)	inflammation, pain, inhibition of platelet aggregation	Beraprost, Treprostinil
	TXA2 receptors (TP_α and TP_β)	TXA_2	inflammation, pain, vasoconstriction, activation of platelet aggregation	Seratrodast, Terutroban
	$CysLT_1$	$LTD_4 > LTC_4 > LTE_4$	bronchoconstriction, chemotaxis, pulmonary inflammation	Pranlukast, Zafirlukast, Montelukast

Reference; J Med Chem. 2017 Jul 13;60(13):5235-5266

Table 2. Fatty acids composition of the high-fat diet (data are expressed as w/w%)

Fatty acids		D12492	D12079B
C2	Acetic	0	0
C4	Butyric	0	0.64
C6	Caproic	0	0.38
C8	Caprylic	0	0.22
C10	Capric	0.01	0.50
C12	Lauric	0.03	0.56
C14	Myristic	0.36	2.00
C14:1	Myristoleic	0	0.30
C15		0.03	-
C16	Palmitic	6.45	5.34
C16:1	Palmitoleic	0.44	0.46
C16:2		0	-
C16:3		0	-
C16:4		0	-
C17		0.12	-
C17:1		0	-
C18	Stearic	3.48	2.44
C18:1	Oleic	11.19	5.26
C18:2	Linoleic	9.45	1.06
C18:3	Linolenic	0.67	0.29
C18:4	Stearidonic	0	0
C20	Arachidic	0.05	0.19
C20:1		0.19	0
C20:2		0.26	-
C20:3		0.04	-
C20:4	Arachidonic	0.09	0
C20:5	Eicosapentaenoic	0	0
C21:5		0	-
C22,	Behenic	0	0
C22:1	Erucic	0	0
C22:4	Clupanodonic	0	0
C22:5	Docosapentaenoic	0.03	0
C22:6	Docosahexaenoic	0	0
C24	Lignoceric	0	0
C24:1		0	-

(%)

Table 3. ***In vitro*** **IC_{50} values (nM) for fatty acid desaturases**

Compound Name	Assay Methods	Species	D5D	D6D	D9D
D5D inhibitor (Compound-326)	Enzyme (hepatic microsomes)	Rat	72	>10 000	>10 000
	Cell-based (HepG2)	Human	22	>10 000	>10 000

Table 4. Sequences of TaqMan primers and probes

Gene	Forward primer	Reverse primer	Probe	Accession number
GPR40/FFA$_1$	5'-GCCCGCTTCAGCCTCTCT-3'	5'-GAGGCAGCCCACGTAGCA-3'	FAM-5'-TCTGCCCTTGGCCATCACAGCCT-3'-TAMRA	NM_005303
GLP-1R	5'-GCAGCCCTGAAGTGGATGTATAG-3'	5'-CTCAGAGAGTCCTGGTAGGAGAG-3'	FAM-5'-ACAGCCGCCCAGCAGCACCAGT-3'-TAMRA	NM_002062
ABCC8	5'-GCTGCCCATCGTTATGAGGG-3'	5'-GAATGTCCTTCCGCACCTGG-3'	FAM-5'-CCTCACCAACTACCAACGGCTCTGCG-3'-TAMRA	NM_000352
GAPDH	5'-TGAAGCAGGCGTCGGAGG-3'	5'-GCTGTTGAAGTCAGAGGAGACC-3'	VIC-5'-CCTCAAGGGCATCCTGGGCTACACTG-3'-TAMRA	NM_002046

FAM, 6-carboxyfluorescein; TAMRA, 6-carboxytetramethylrhodamine;

Table 5. Clinical profiles of islet donors

Experiment	Donor No.	Age(years)	Sex(M/F)
Gene analysis (Fig. 4)	1	65	M
	2	55	M
	3	43	M
	4	52	M
Hormone secretion assay (Table S3, Fig. 5)	5	33	M
	6	54	-
	7	51	M
	8	57	F
Intracellular Ca^{2+} measurements (Fig. 6)	7	51	M
	8	57	F
	9	66	M

M; Male, F; Female

Table 6. Summary of the results of static incubation assay in human islets (from 4 organ donors)

		1 mM Glucose		16 mM Glucose				
	No.		GPR40 ago.		GPR40 ago.			GLP-1
(% of content/h)		-	(1 μM)	-	(0.3 μM)	(1 μM)	(3 μM)	(10 nM)
Insulin	5	0.27±0.02	0.35±0.02[a]	0.45±0.02[d]	0.83±0.11[e]	1.06±0.09[e]	0.78±0.06[e]	0.93±0.08[a]
	6	1.68±0.23	1.48±0.18	2.90±0.28[c]	4.79±0.42[e]	4.18[e]	-	6.26±1.13
	7	0.44±0.03	0.45±0.10	1.76±0.18[b]	-	1.78±0.14	-	2.76±0.21[a]
	8	0.05±0.01	0.04±0.00	0.29±0.01[d]	0.33±0.04	0.39±0.10	0.49±0.09	0.40±0.04
Glucagon	5	2.49±0.26	2.44±0.24	1.62±0.10[a]	1.93±0.22	1.81±0.35	1.68±0.49	1.75±0.12
	6	0.81±0.19	0.56±0.11	0.59±0.02	0.84±0.14	0.38	-	0.46±0.10
	7	1.19±0.21	1.87±0.41	1.13±0.15	-	1.16±0.30	-	1.79±0.24
	8	1.02±0.19	0.95±0.11	0.72±0.13	0.79±0.20	0.68±0.11	0.77±0.10	0.59±0.11

Human islets had been pre-incubated for 1 h at 1 mM glucose. Following the pre-incubation, these islets were incubated with the assay buffer containing 1 or 16 mM glucose with or without test substances for 1 h. Insulin (upper panel) and glucagon (lower panel) secretion were shown as % of content/h. Data are expressed as mean ± *SEM* (n=2-4). [a] $p \leq 0.05$, [b] $p \leq 0.01$ vs. 1 mM glucose control (Aspin Welch test), [c] $p \leq 0.05$, [d] $p \leq 0.01$, vs. 16 mM glucose control (Student's *t*-test). [e] $p \leq 0.025$, vs. 16 mM glucose control (one-tailed Williams' test).

Figures

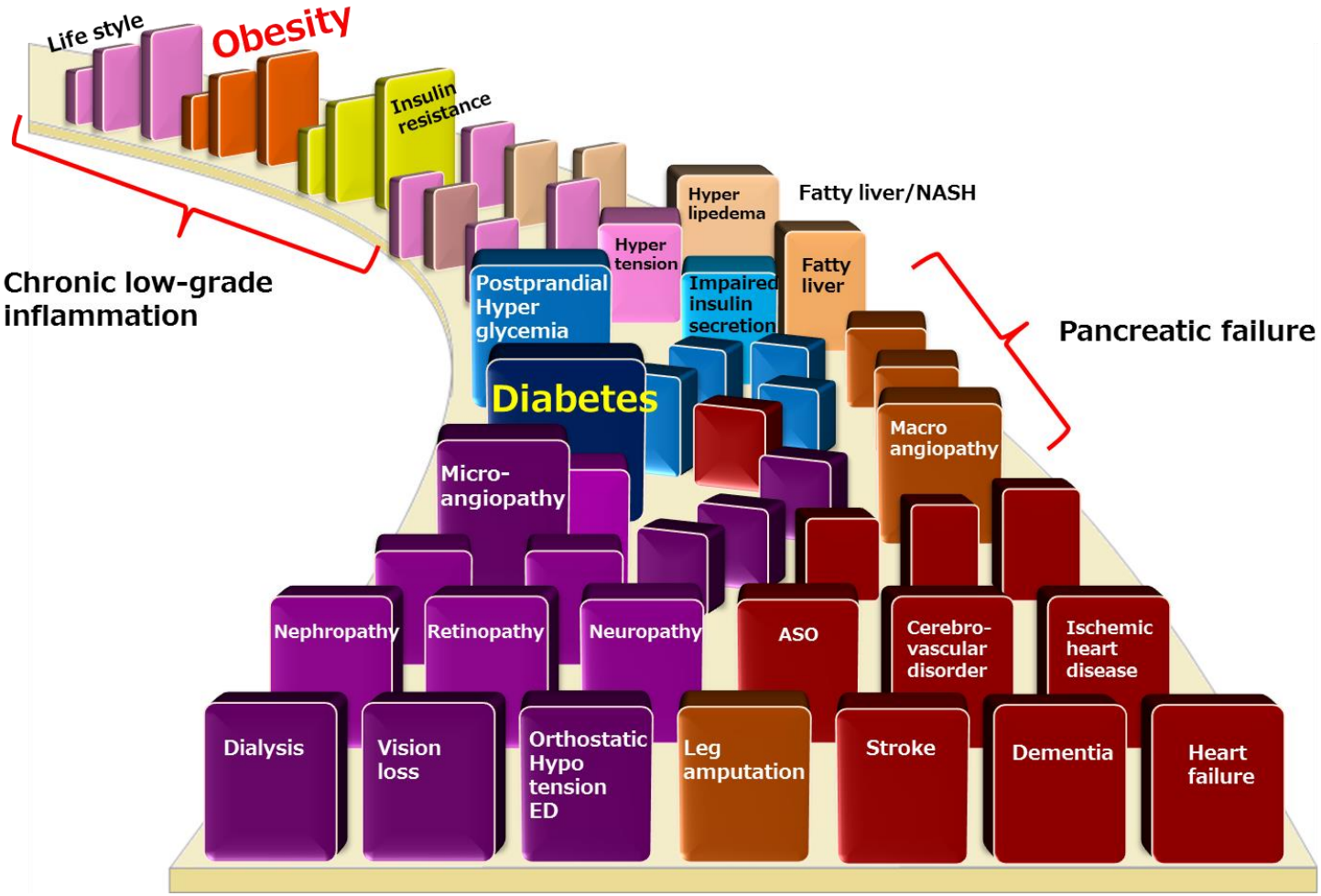

Fig. 1 The concept of metabolic domino

Reference; Itoh H. Drugs Today (Barc). 2006; 42: Suppl C9-16

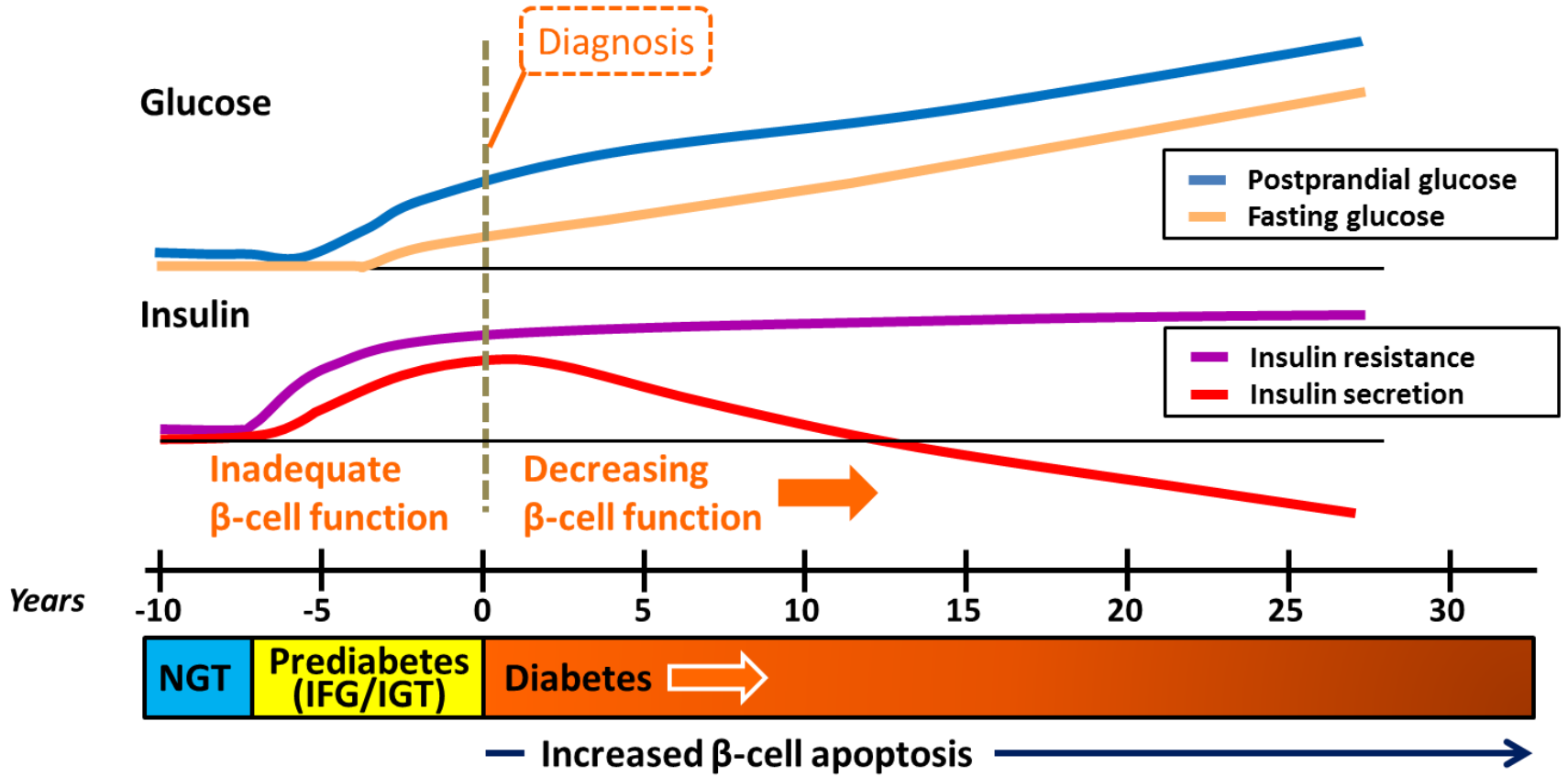

Fig. 2 Changes of insulin secretion during the progression T2DM

Reference; Adapted from T2DM BASICS. International Diabetes Center: 2000.

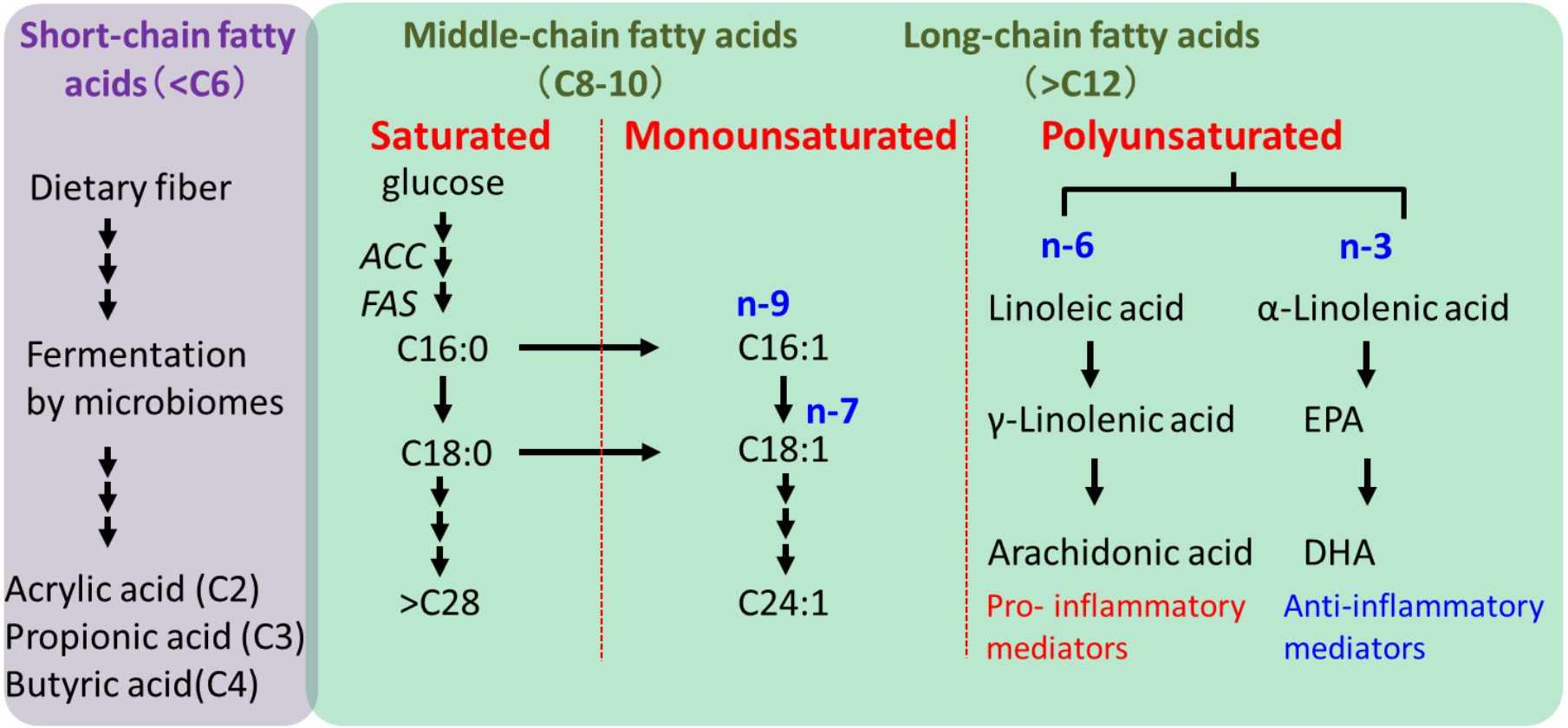

Fig. 3 Classification and *de novo* fatty acids synthesis

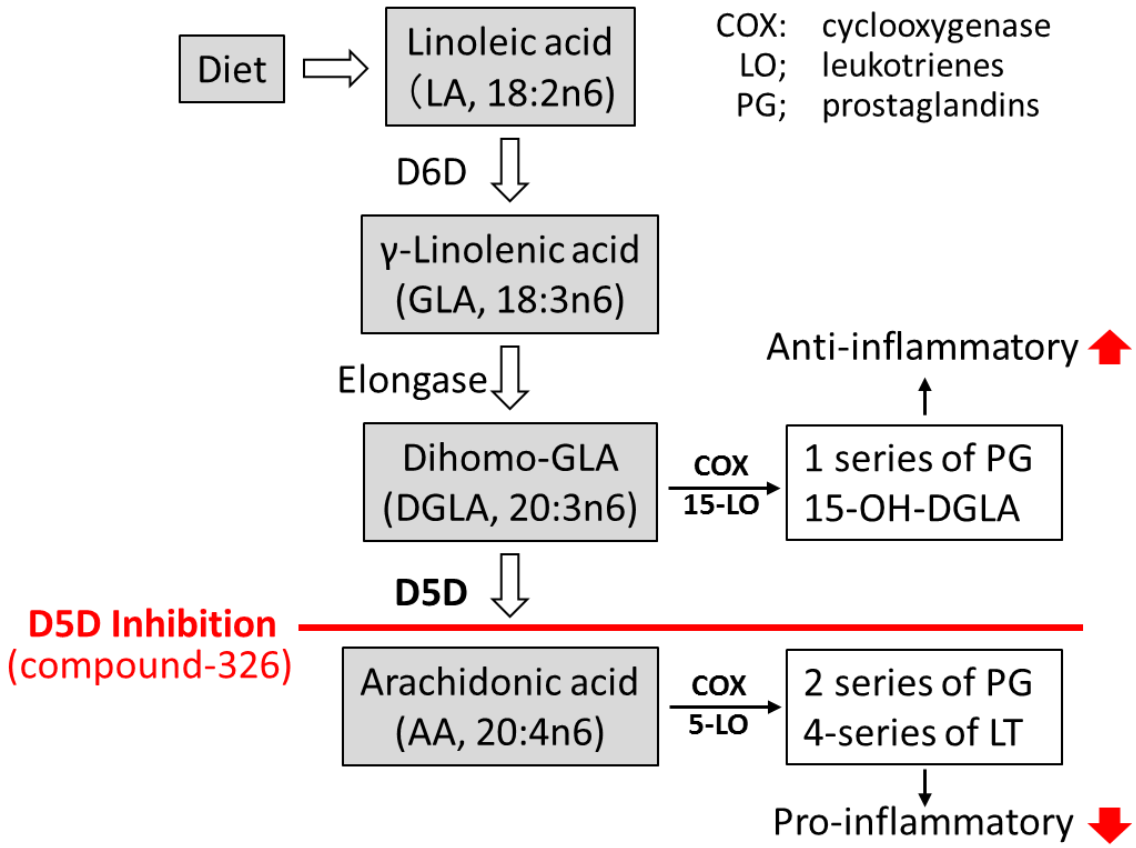

Fig. 4 Biosynthesis pathway of n-6 polyunsaturated fatty acids

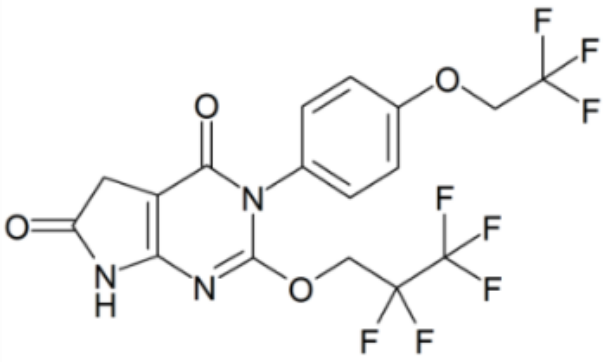

Fig. 5 Structure of D5D inhibitor; compound-326

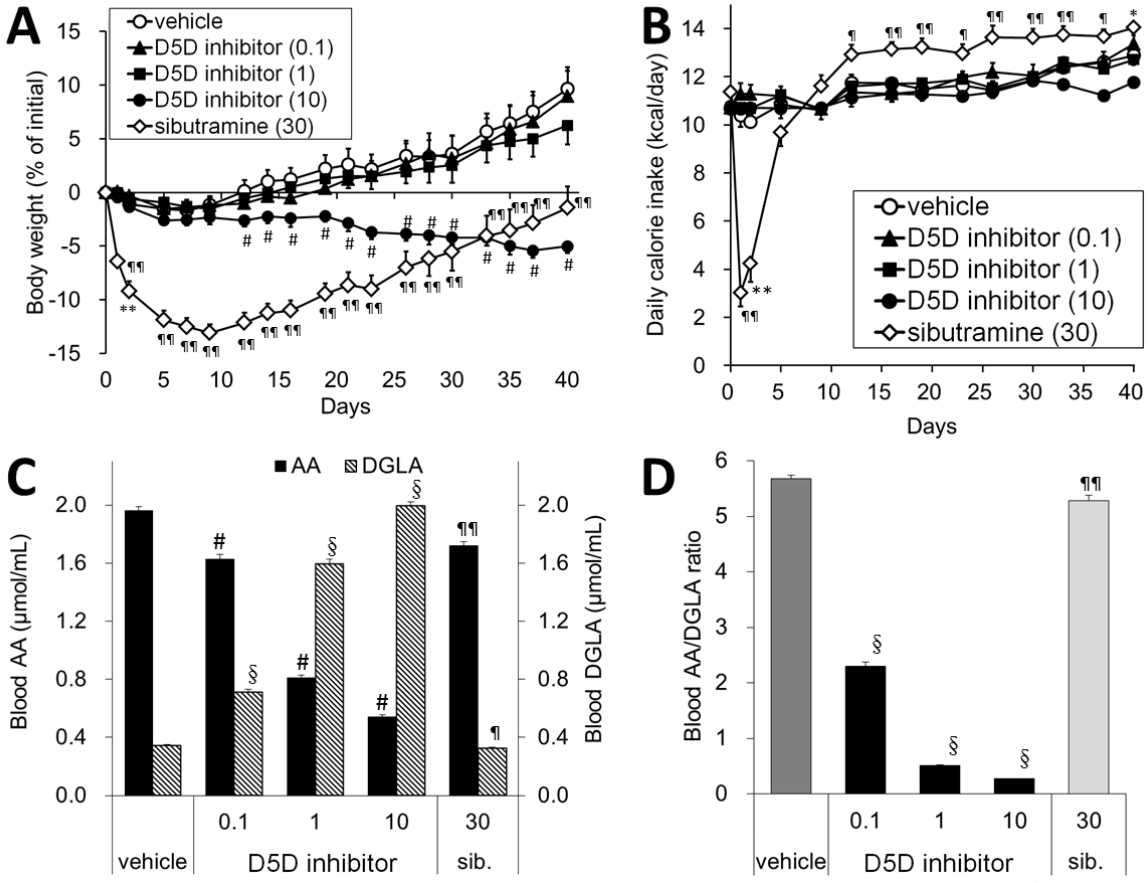

Fig. 6 Effects of chronic treatment with D5D inhibitor on BW, calorie intake, and blood PD markers in DIO mice

DIO mice (initial BW; 31.1±1.6 g) were treated with D5D inhibitor (0.1, 1, and 10 mg/kg), 30 mg/kg sibutramine, or vehicle p.o. for 6 weeks. (**A**) Changes in BW from initial value. (**B**) Daily calorie intake during the study. (**C**) Changes in blood AA and DGLA concentrations after 6-week treatment. (**D**) Changes in the blood AA to DGLA ratio after 6-week treatment. Data are expressed as mean ± *SEM* (n=7). # $p \leq 0.025$ vs. DIO vehicle by Williams' test. § $p \leq 0.025$ vs. DIO vehicle by Shirley-Williams test. * $p \leq 0.05$, ** $p \leq 0.01$ vs. DIO vehicle by Aspin-Welch test. ¶ $p \leq 0.05$, ¶¶ $p \leq 0.01$ vs. DIO vehicle by Student's *t*-test.

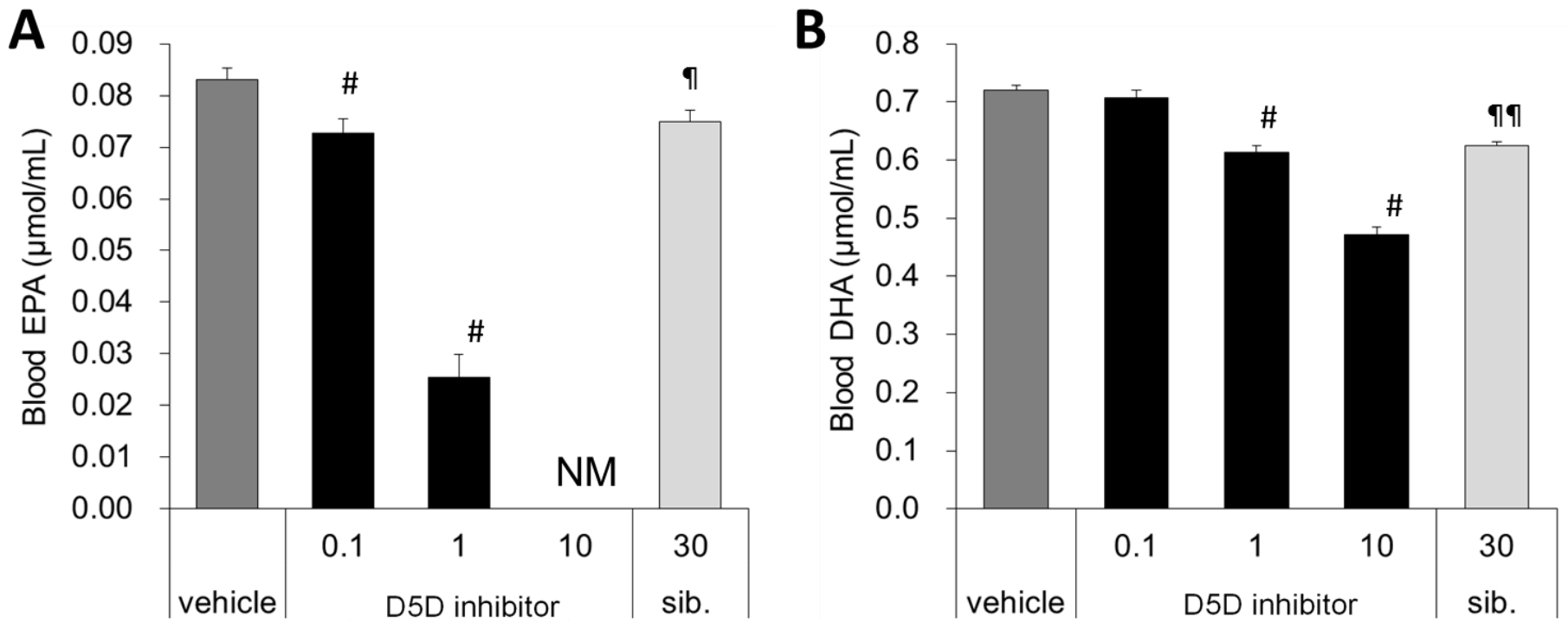

Fig. 7 Effects of chronic treatment with D5D inhibitor on blood EPA and DHA levels in DIO mice

DIO mice (initial BW; 31.1±1.6 g) were treated with D5D inhibitor (0.1, 1, and 10 mg/kg), 30 mg/kg sibutramine, or vehicle p.o. for 6 weeks. (**A**) Changes in blood EPA concentrations after 6-week treatment. (**B**) Changes in blood DHA concentrations after 6-week treatment. NM stands for note measurable. Data are expressed as mean ± *SE*M (n=7). # $p \leq 0.025$ vs. DIO vehicle by Williams' test. ¶ $p \leq 0.05$, ¶¶ $p \leq 0.01$ vs. DIO vehicle by Student's *t*-test.

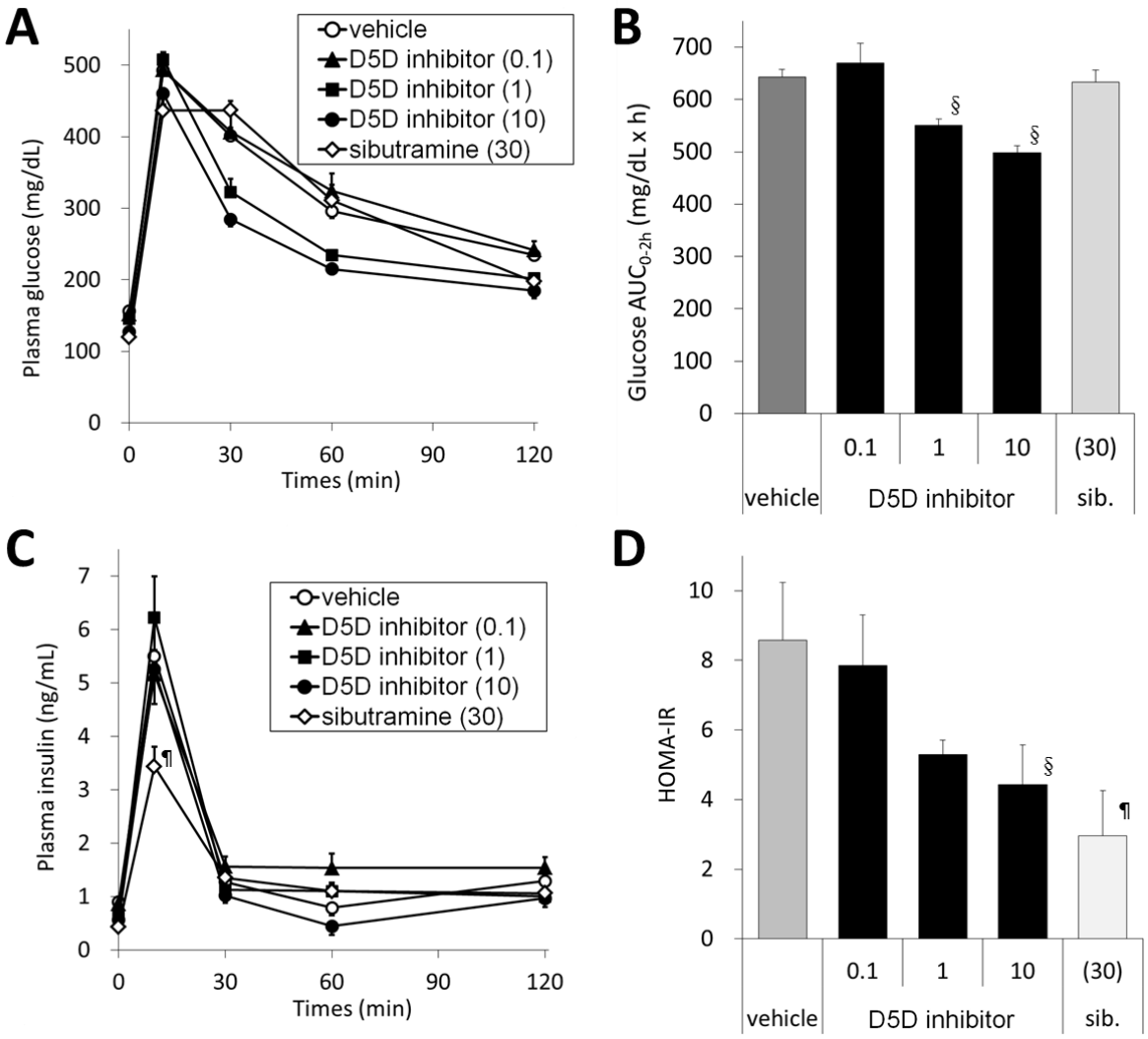

Fig. 8 Effects of chronic treatment with D5D inhibitor on plasma glucose and insulin during an OGTT, and HOMA-IR in DIO mice

Oral glucose tolerance test (OGTT) was performed after chronic treatment with D5D inhibitor for 6 weeks in DIO mice. (**A**) Changes in plasma glucose levels. (**B**) Effect on plasma glucose AUC. (**C**) Changes in plasma insulin levels. (**D**) Effect on HOMA-IR. Data are expressed as mean ± *SEM* (n=7). § $p \leq 0.025$ vs. DIO vehicle by Shirley-Williams test. ¶ $p \leq 0.05$ vs. DIO vehicle by Student's *t*-test.

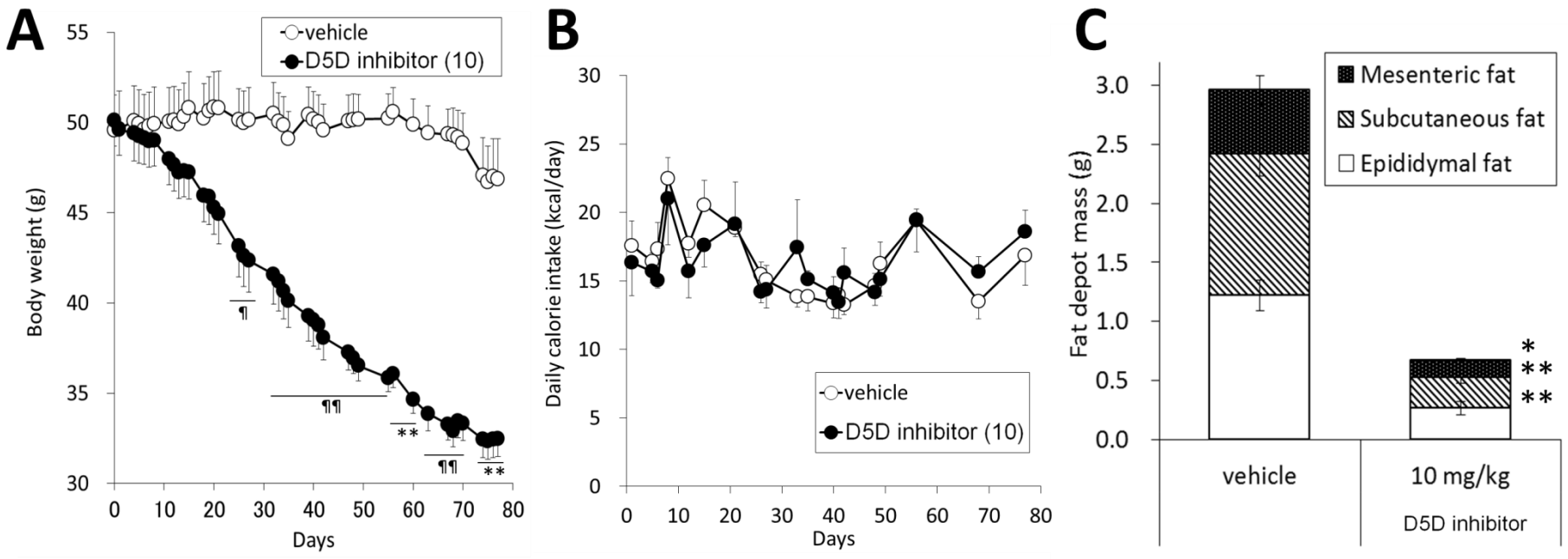

Fig. 9 Effects of chronic treatment with D5D inhibitor on BW, calorie intake, and fat mass in DIO mice

DIO mice were treated with 10 mg/kg D5D inhibitor, p.o., for 11 weeks. (**A**) Changes in BW. (**B**) Changes in daily calorie intake. (**C**) Weights of different body fat depots after 11-week treatment. Data are expressed as mean ± *SEM* (n=7). * $p \leq 0.05$, ** $p \leq 0.01$ vs. DIO vehicle by Aspin-Welch test. ¶ $p \leq 0.05$, ¶¶ $p \leq 0.01$ vs. DIO vehicle by Student's *t*-test.

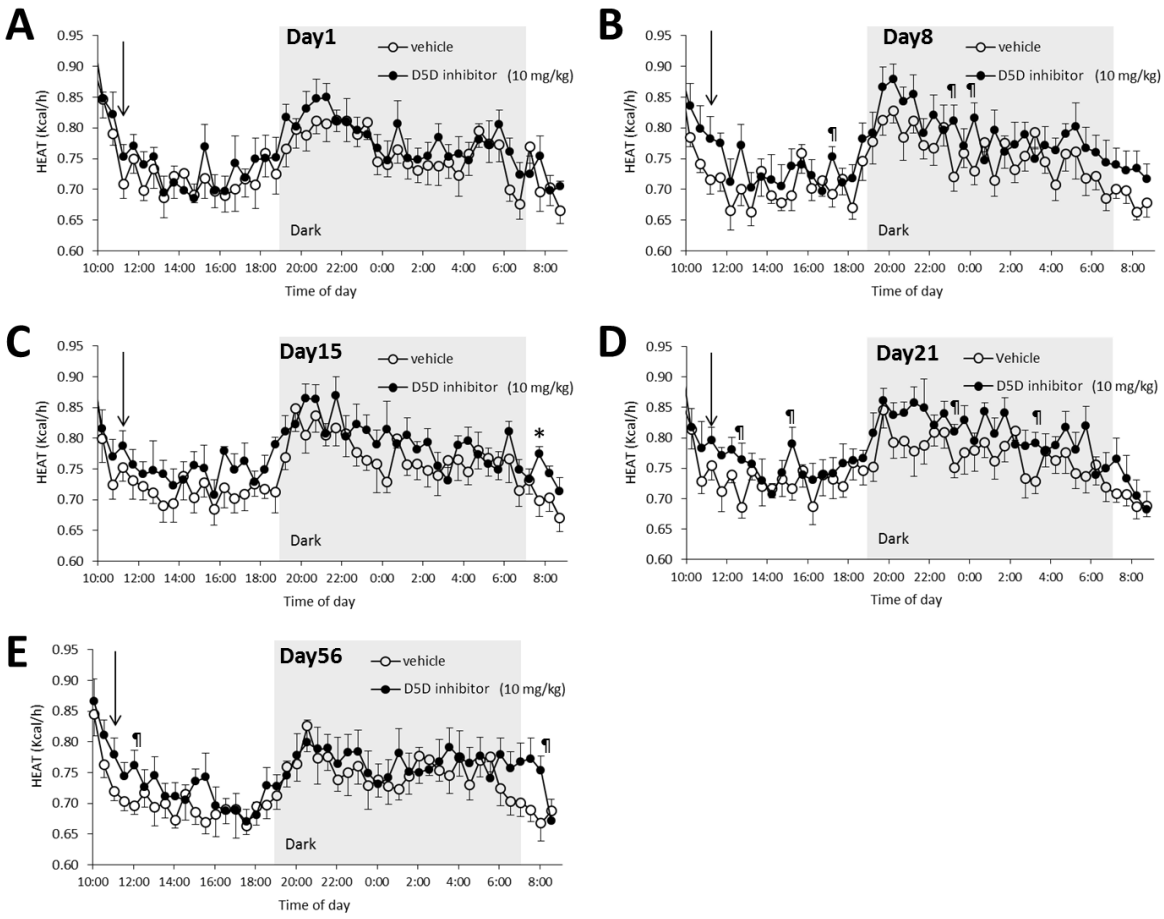

Fig. 10 Effect of chronic treatment with D5D inhibitor on energy expenditure in DIO mice

Energy expenditure (EE) was monitored on days 1 (**A**), 8 (**B**), 15 (**C**), 21 (**D**), and 56 (**E**) during chronic dosing study indicated in Fig 9. Arrows indicate the timing of drug administration. Data are expressed as mean ± *SEM* (n=7). * $p \leq 0.05$ vs. DIO vehicle by Aspin-Welch test. ¶ $p \leq 0.05$ vs. DIO vehicle by Student's *t*-test.

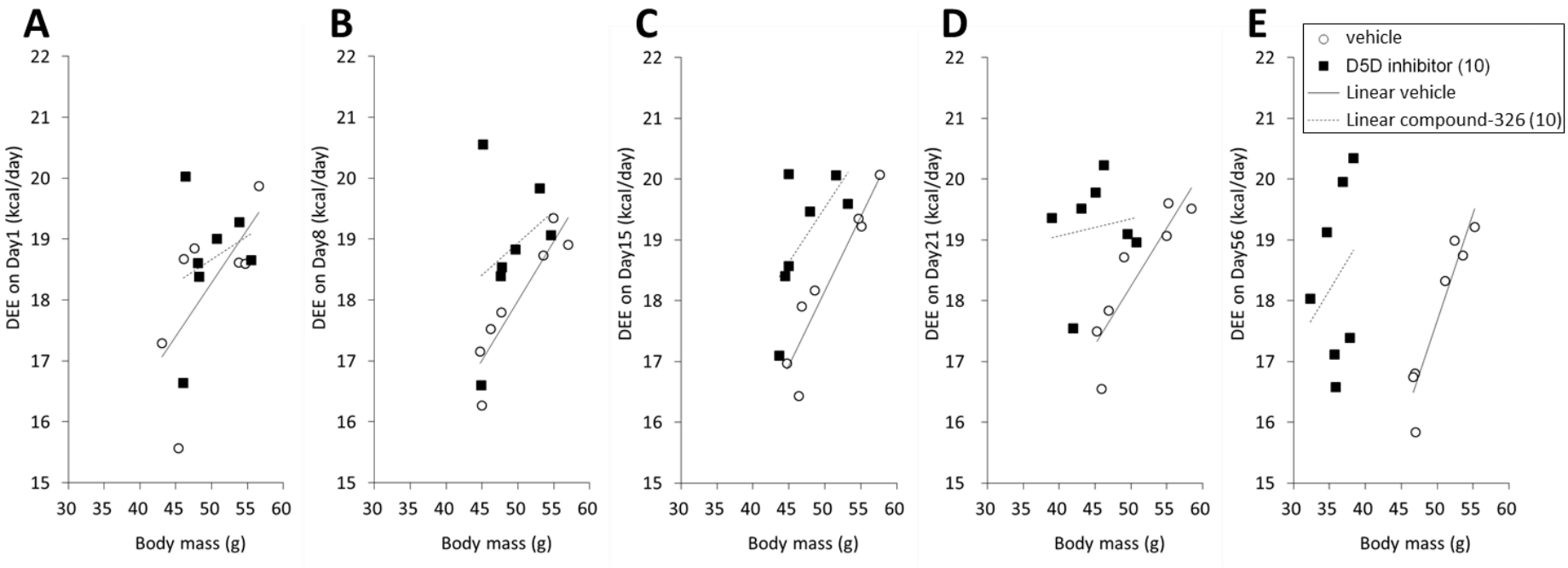

Fig. 11 Effect of chronic treatment with D5D inhibitor on energy expenditure in DIO mice

Daily energy expenditure (DEE) was monitored on days 1 (**A**), 8 (**B**), 15 (**C**), 21 (**D**), and 56 (**E**) during the study indicated in Fig 10.

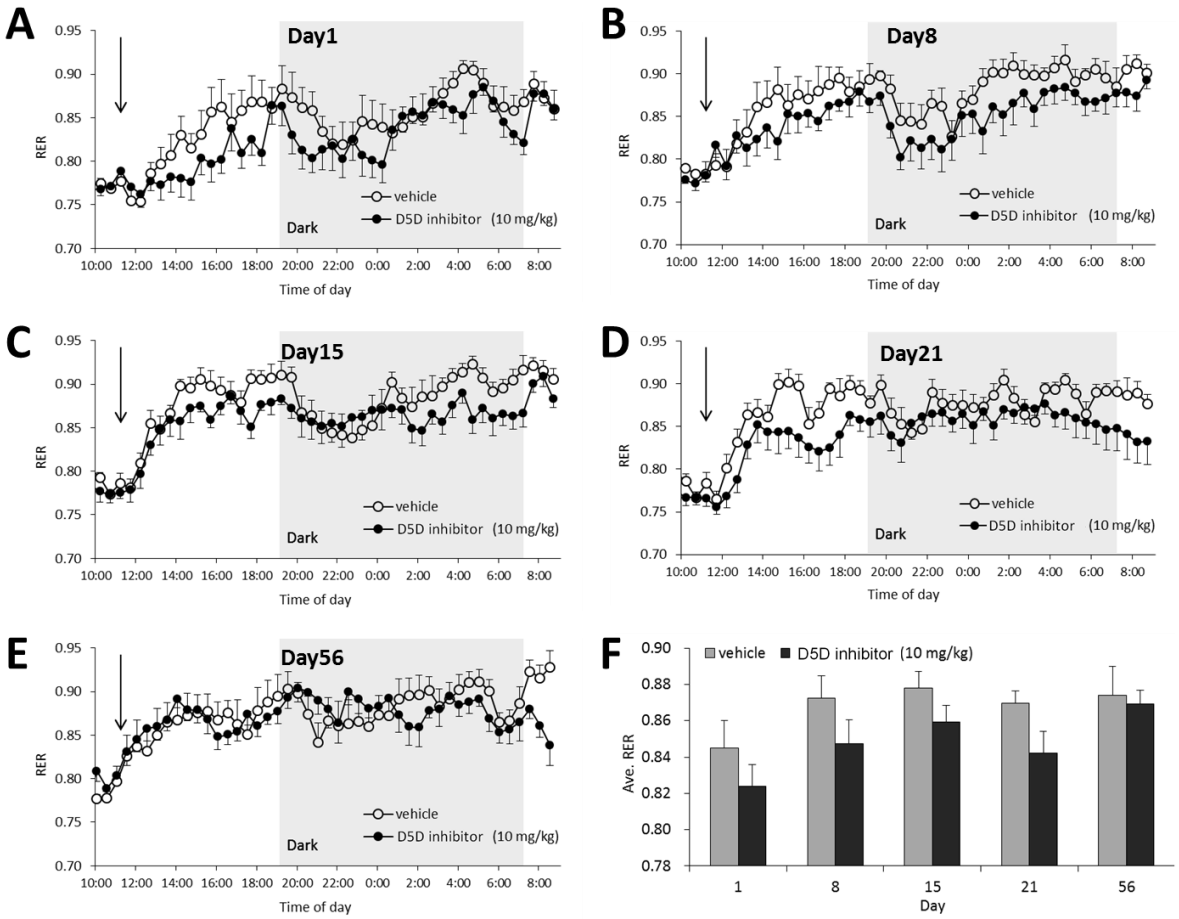

Fig. 12 Effect of chronic treatment with D5D inhibitor on respiratory exchange ratio in DIO mice

Respiratory exchange ratio (RER) was monitored on days 1 (**A**), 8 (**B**), 15 (**C**), 21 (**D**), and 56 (**E**) during chronic dosing study indicated in Fig 9. (**F**) Changes in averaged RER. Arrows indicate the timing of drug administration. Data are expressed as mean ± *SEM* (n=7).

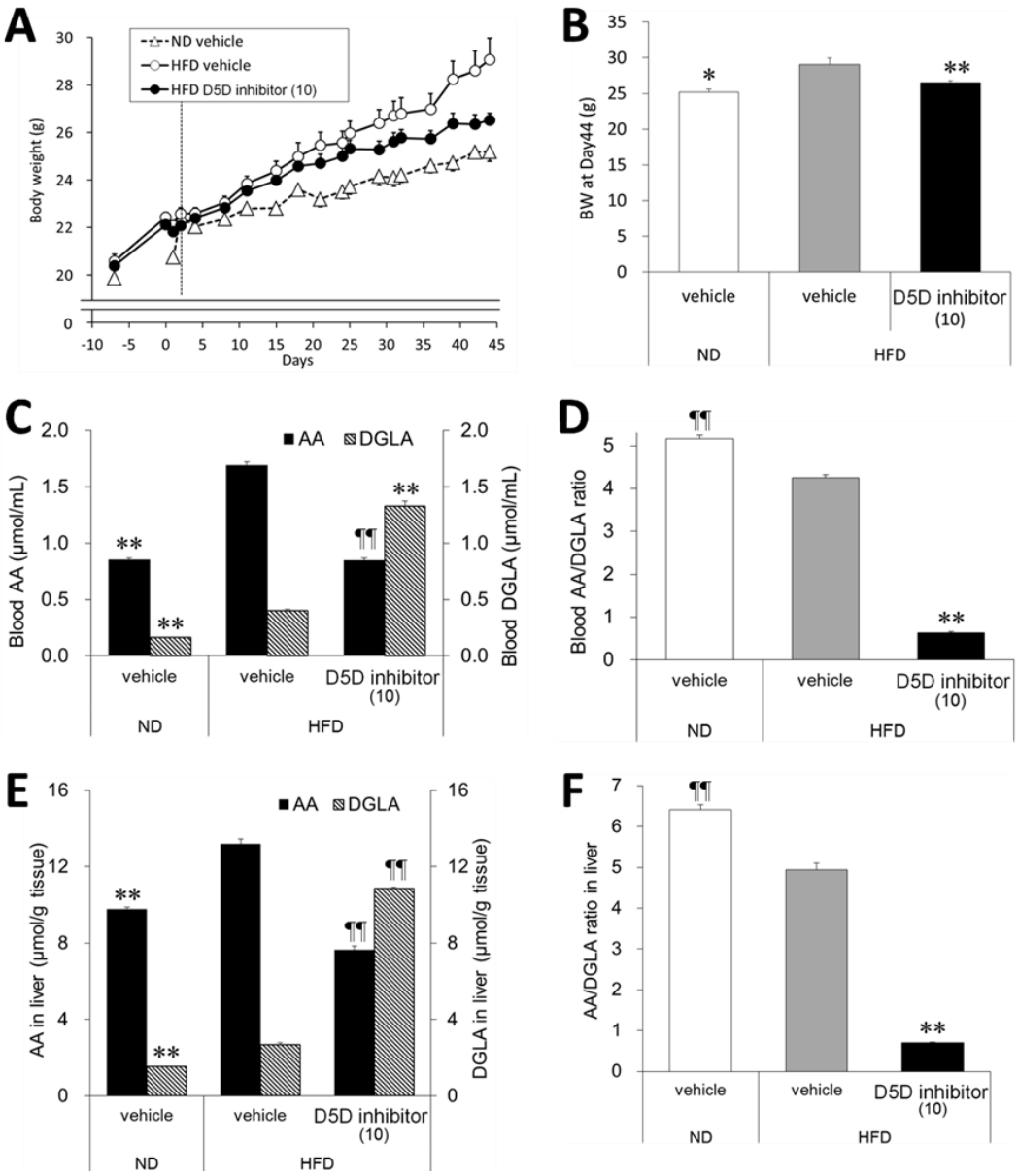

Fig. 13 Effects of D5D inhibitor on BW and AA and DGLA levels within the blood as well as liver in DIO mice

Chronic administration of D5D inhibitor (10 mg/kg) significantly decreased BW in DIO mice. In these mice, increase in DGLA and decrease in AA in the blood as well as liver were observed after 6-week treatment with compound-326. (**A**) BW changes during the study. (**B**) BW at Day44. (**C**) Levels of AA and DGLA in the blood. (**D**) AA to DGLA ratio in the blood. (**E**) Levels of AA and DGLA in the liver. (**F**) AA to DGLA ratio in the liver. Data are expressed

as mean ± *SEM* (n=8-9). * $p \leq 0.05$, ** $p \leq 0.01$ vs. DIO vehicle by Aspin-Welch test. ¶¶ $p \leq 0.01$ vs. DIO vehicle by Student's *t*-test.

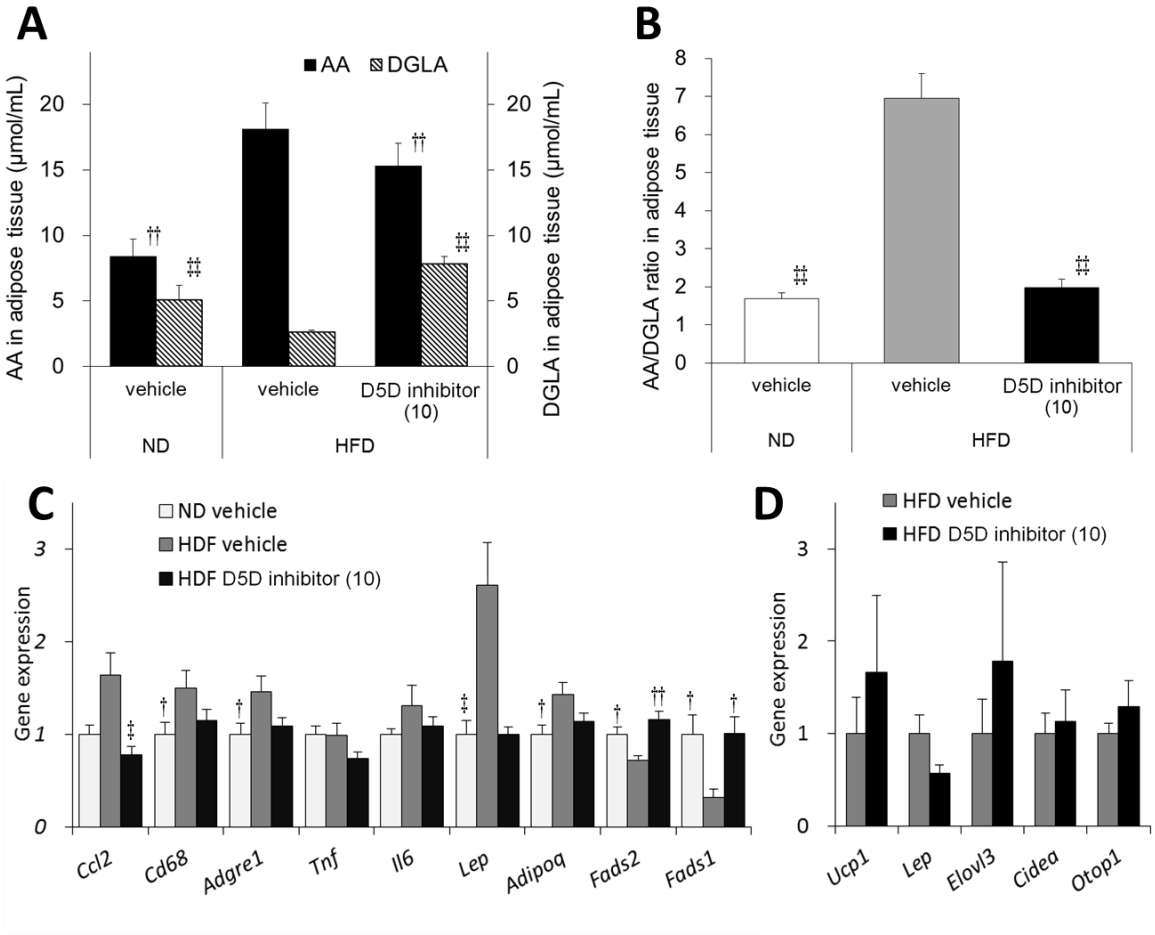

Fig. 14 Effects of chronic treatment with D5D inhibitor on PD markers and gene expression in WAT in DIO mice

HFD-fed DIO mice were treated with D5D inhibitor (10 mg/kg), p.o. for 6 weeks. Mice fed a normal diet (ND) were used as normal reference. (**A**) Levels of AA and DGLA in epididymal adipose tissue. (**B**) AA to DGLA ratio in epididymal adipose tissue. RT-qPCR was performed in epididymal (**C**) and subcutaneous fat tissues (**D**) after 6-week treatment. Data are expressed as mean ± *SEM* (n=8-9). * $p \leq 0.05$, ** $p \leq 0.01$ vs. DIO vehicle by Aspin-Welch test. ¶ $p \leq 0.05$, ¶¶ $p \leq 0.01$ vs. DIO vehicle by Student's *t*-test.

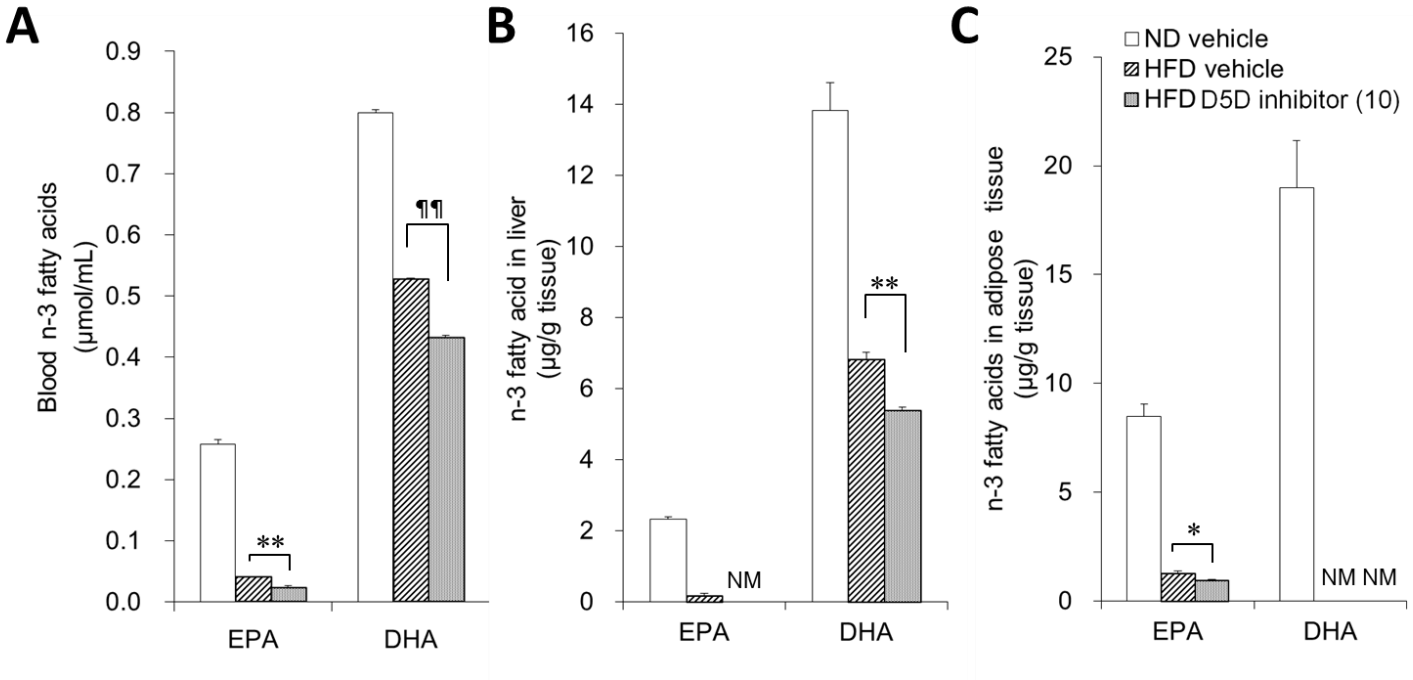

Fig. 15 Effects of chronic treatment with D5D inhibitor on blood and tissue EPA and DHA levels in HFD-fed mice

HFD-fed mice were treated with D5D inhibitor (10 mg/kg), p.o. for 6 weeks. Mice fed a normal diet (ND) were used as normal reference. (**A**) Levels of EPA and DHA in the blood. (**B**) Levels of EPA and DHA in epididymal adipose tissue. (**C**) Levels of EPA and DHA in epididymal adipose tissue. NM stands for note measurable. Data are expressed as mean ± *SEM* (n=8-9). * $p \leq 0.05$ and ** $p \leq 0.01$ vs. DIO vehicle by Aspin-Welch test. ¶¶ $p \leq 0.01$ vs. DIO vehicle by Student's *t*-test.

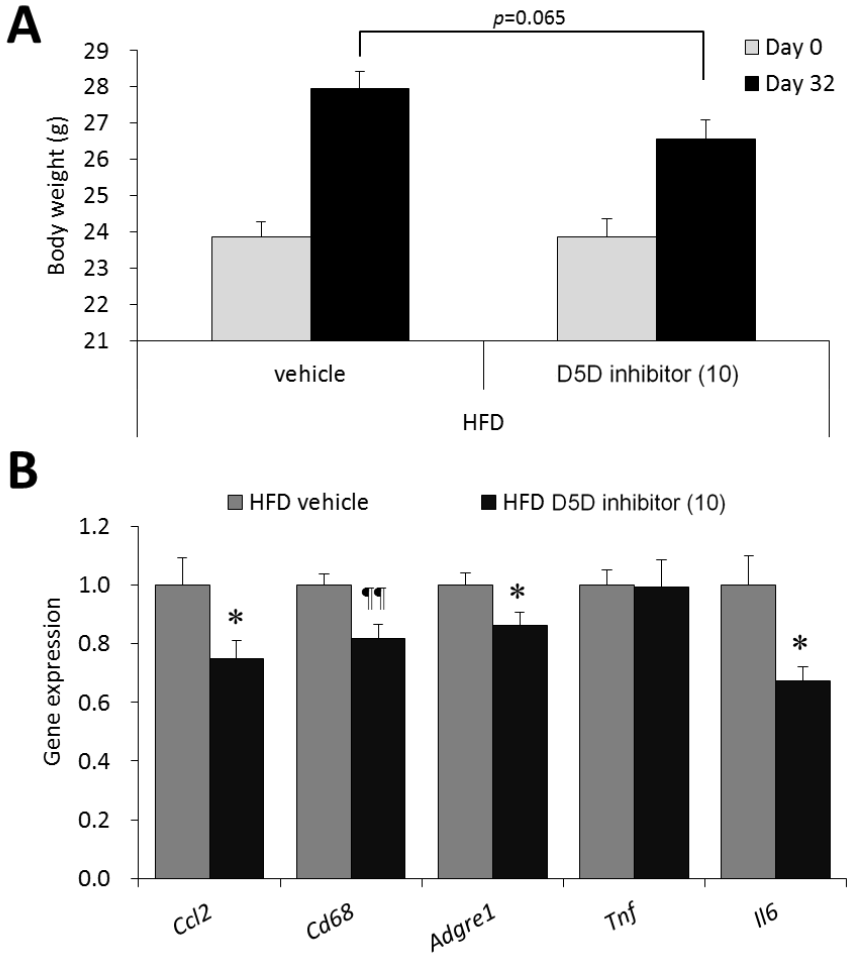

Fig. 16 Effects of D5D inhibitor on WAT gene expression in satellite DIO mice (Day32)

In 6 weeks administration study of D5D inhibitor (10 mg/kg), satellite animals were prepared to evaluate the gene expression levels in epididymal fat at the intermediate point (day 32). Mice fed a HFD (D12079B; Research diets, Inc.) from 5 weeks of age were divided into 2 groups at the age of 8 weeks (11 animals per group), and were administered 10 mg/kg compound-326 or vehicle for 32 days. After the treatment period, mice were sacrificed and epididymal fats were harvested for mRNA analysis. (**A**) Compound-326 administration showed a trend towards BW loss in DIO mice. (**B**) RT-qPCR was performed in epididymal fat tissue after 32 days treatment. Data are expressed as mean ± *SEM* (n=11). * $p \leq 0.05$ vs. DIO vehicle by Aspin-Welch test. ¶¶ $p \leq 0.01$ vs. DIO vehicle by Student's *t*-test.

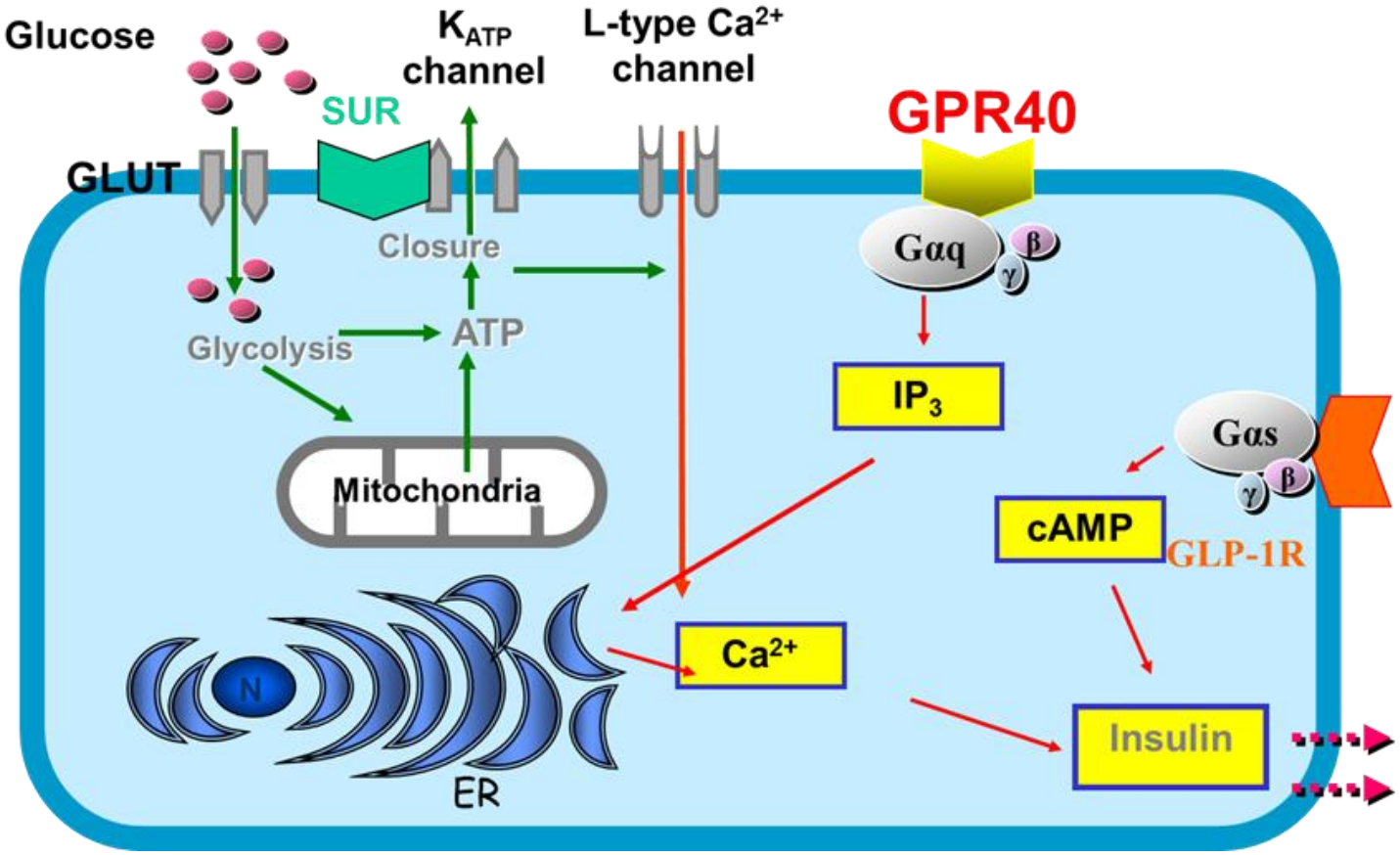

Fig. 17 Presumed mechanism of insulin secretion via GPR40 in pancreatic beta cell

PLC, phospholipase C; IP3, inositol triphosphate; DAG, diacylglycerol; PKC, protein kinase C.

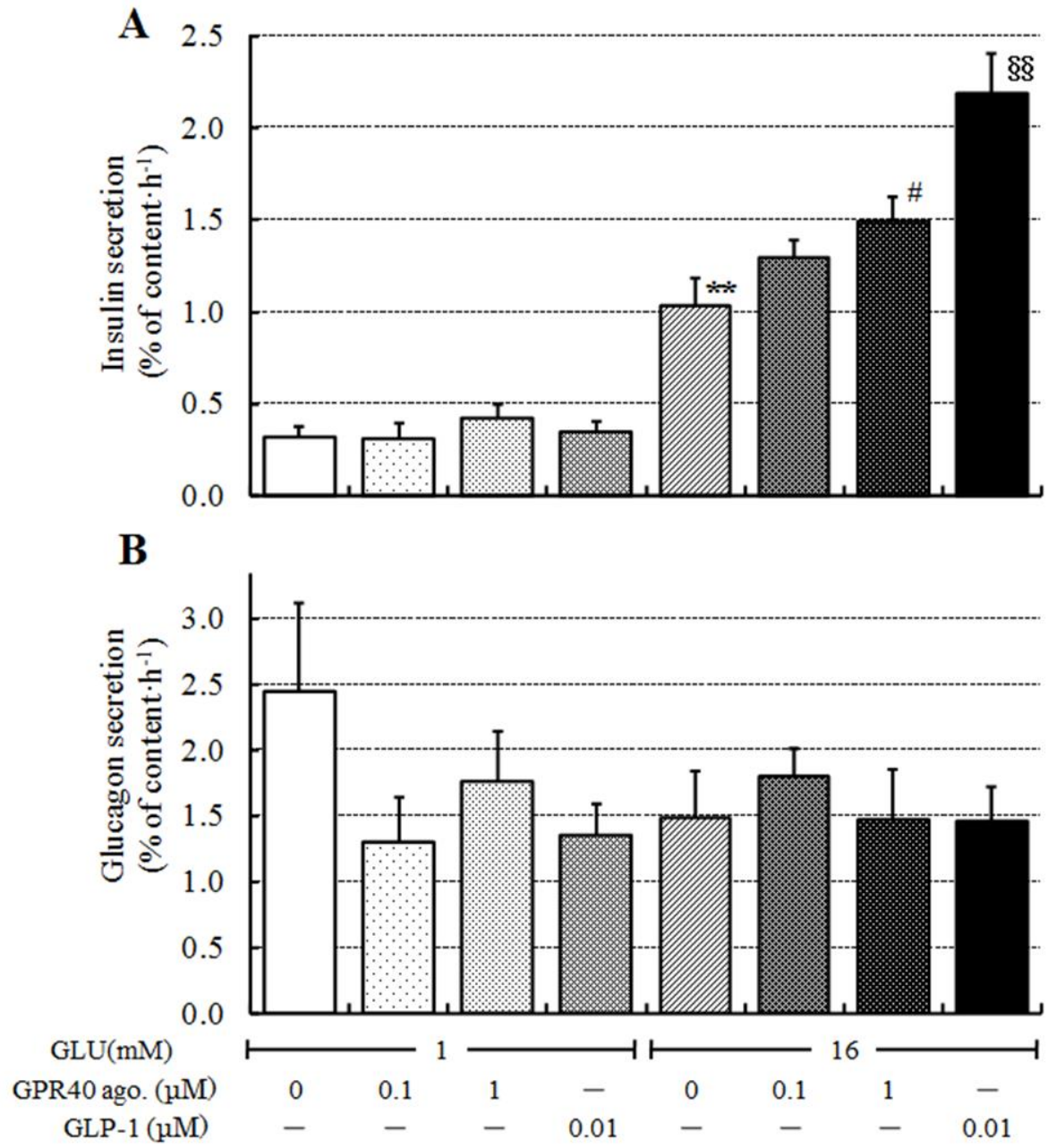

Fig. 18 Effects of GPR40 agonist on insulin and glucagon secretion in rat islets

Isolated rat islets were incubated with the assay buffer containing 1 or 16 mM glucose with or without test substances for 1 h. Insulin (A) and glucagon (B) secretion are quoted as % of content/h. Data are expressed as mean ± *SEM* (n=6). ** $p \leq 0.01$ vs. 1 mM glucose control (Aspin-Welch test), §§ $p \leq 0.01$ vs. 16 mM glucose control (Student's *t*-test); # $p \leq 0.025$ vs. 16 mM glucose control (one-tailed Williams' test).

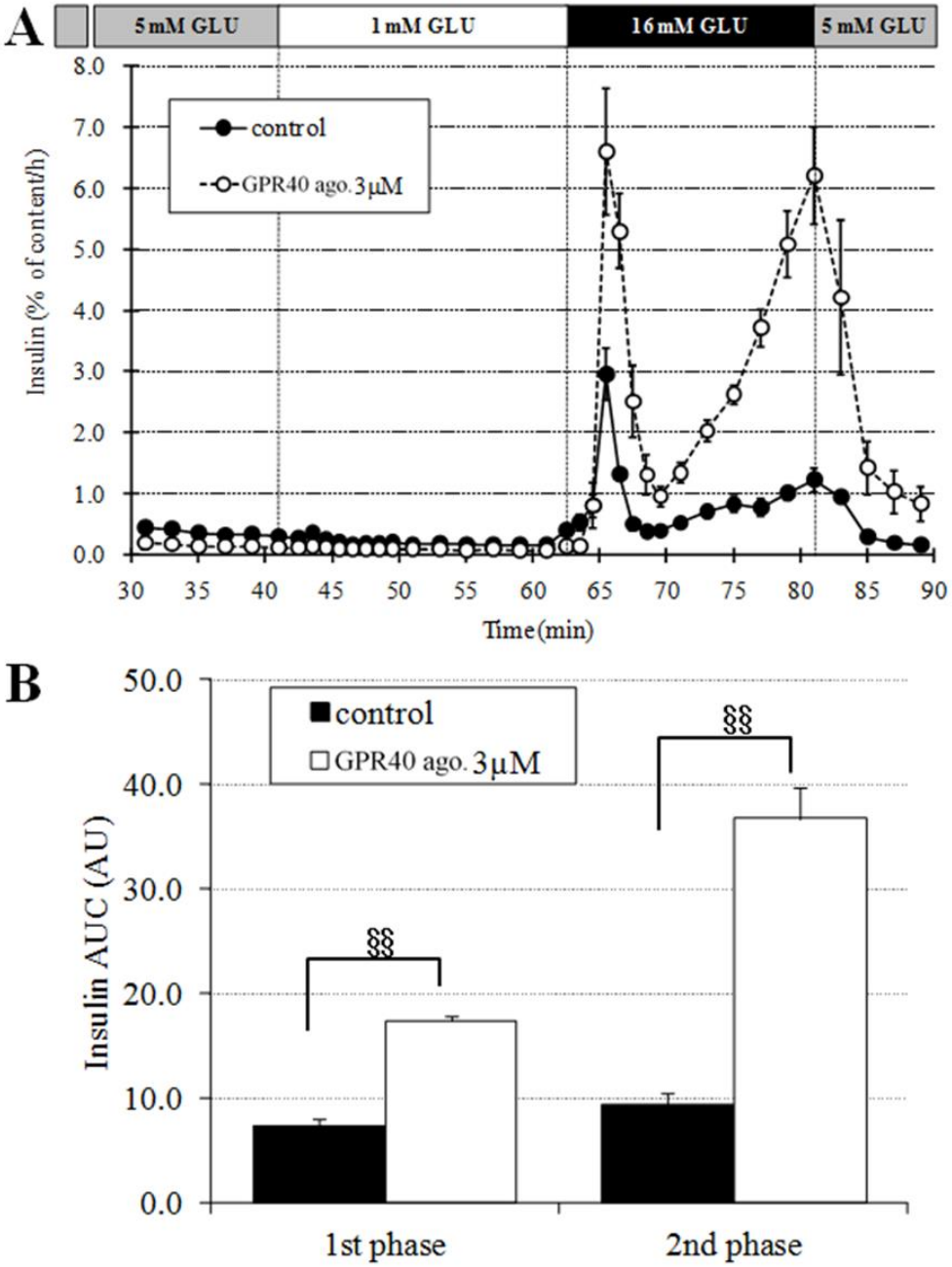

Fig. 19 Effect of GPR40 agonist on insulin secretion in perifused rat islets

(A) Isolated rat islets were perifused with 1, 5 or 16 mM glucose with (○) or without GPR40 agonist (3 μM; ●). The perifusate was collected every 1 or 2 min. Secreted insulin levels are shown as % of content/h. (B) AUC of secreted insulin during 1st and 2nd phase. Data are expressed as mean ±*SEM* (n=3). §§ $p \leq 0.01$ vs. 16 mM glucose control (Student's *t*-test). AU stands for arbitrary units.

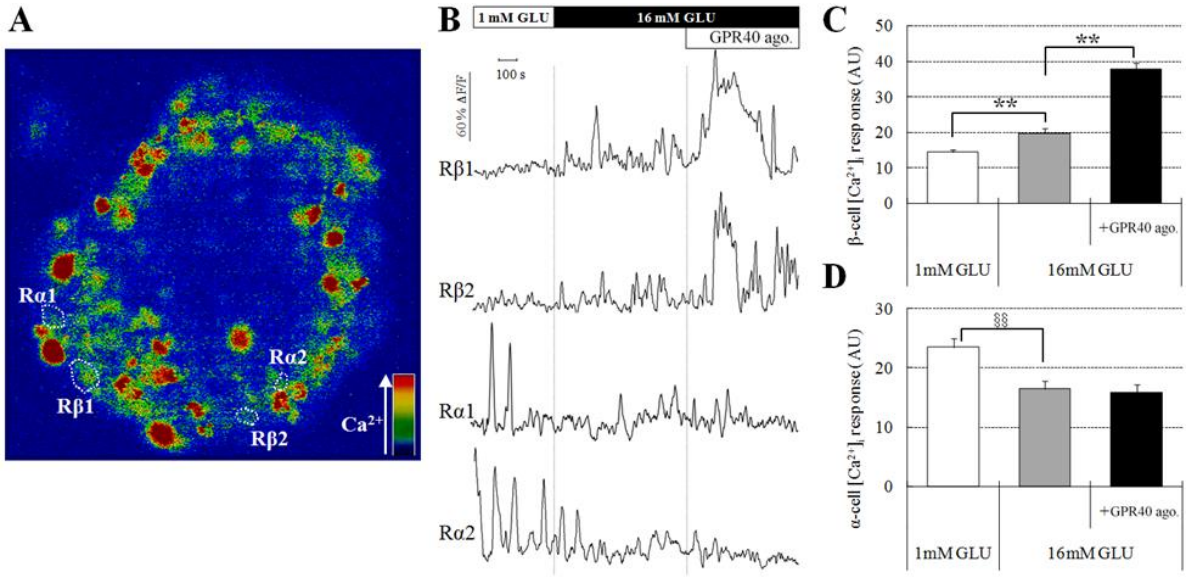

Fig. 20 Effects of GPR40 agonist on the intracellular Ca^{2+} response of single β and α cells within intact rat islets

(A) Color image of rat islet located with the Ca^{2+}-sensitive dye Fluo-4 at the beginning of Ca^{2+} recording. (B) Records of fluorescence intensity versus time from the cells indicated in panel A. Rβ1, 2 and Rα1, 2 are the representative $[Ca^{2+}]_i$ response from single β- and α-cells, respectively, exposed to 1 mM glucose, 16 mM glucose and 16 mM glucose plus 3 μM GPR40 agonist as indicated above the traces. (C) Summary of the $[Ca^{2+}]_i$ response from 43 single β-cells within 3 independent islets and expressed as mean ±*SEM* (D) Summary of $[Ca^{2+}]_i$ response from 23 single α-cells within 3 independent islets, expressed as mean ±*SEM*. ** $p \leq 0.01$ vs. 1 or 16 mM glucose control (Aspin-Welch test); §§ $p \leq 0.01$ vs. 16 mM glucose control (Student's *t*-test). AU stands for arbitrary units.

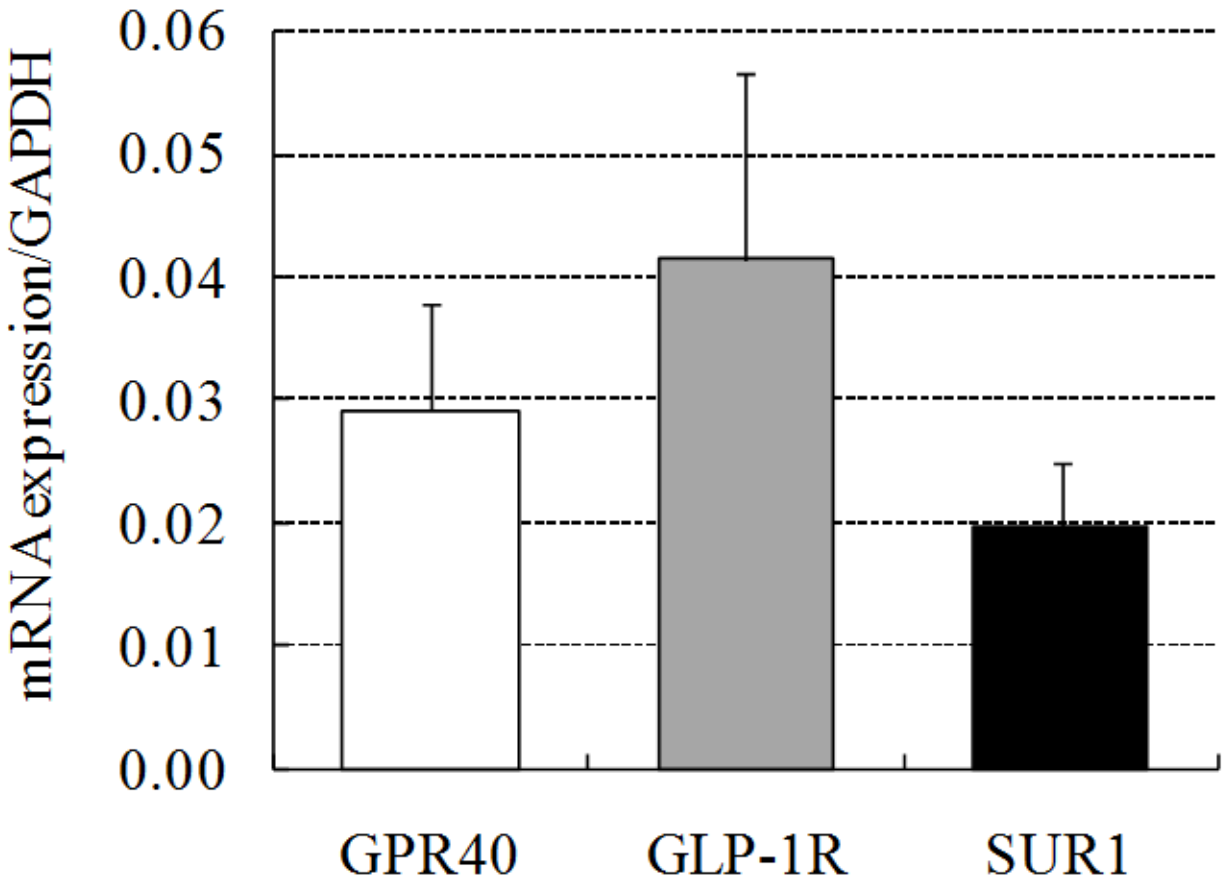

Fig. 21 Comparison of gene expression levels of GPR40, GLP-1R and SUR1 in human islets

The relative mRNA expressions for an internal control GAPDH are expressed as mean and *SEM* (n=4).

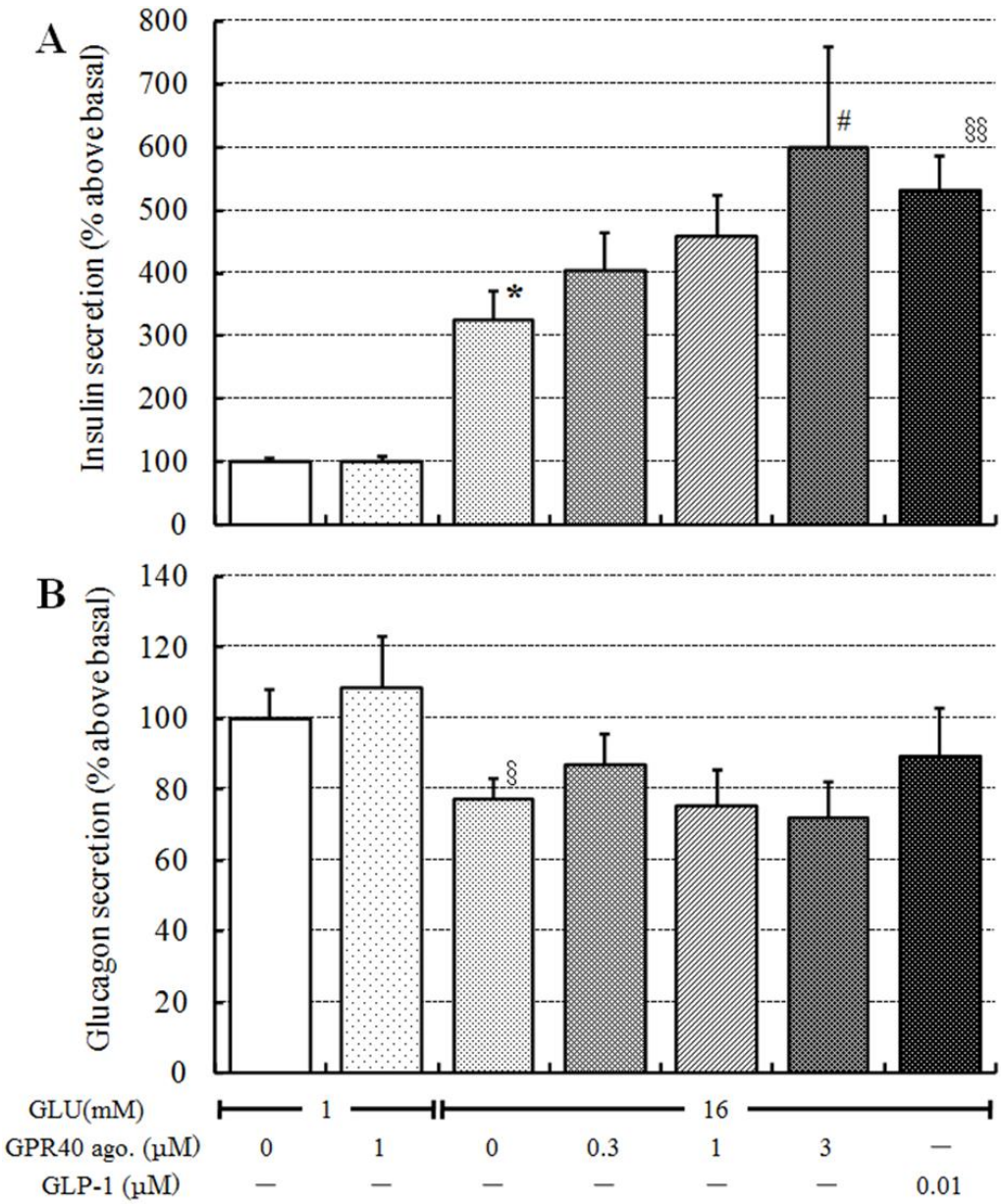

Fig. 22 Effects of GPR40 agonist on insulin and glucagon secretion in human islets

The mean value of hormone levels for 1 mM glucose control equals 100%, and all data are expressed as percentage from basal. Data are expressed as mean ± *SEM* (n=6-13). * $p \leq 0.05$ vs. 1 mM glucose control (Aspin-Welch test); § $p \leq 0.05$ vs. 1 mM glucose control, §§ $p \leq 0.01$ vs. 16 mM glucose control (Student's *t*-test); # $p \leq 0.025$ vs.16 mM glucose control (one-tailed Williams' test). Data of the separate experiments (individual donors) are provided in table 6.

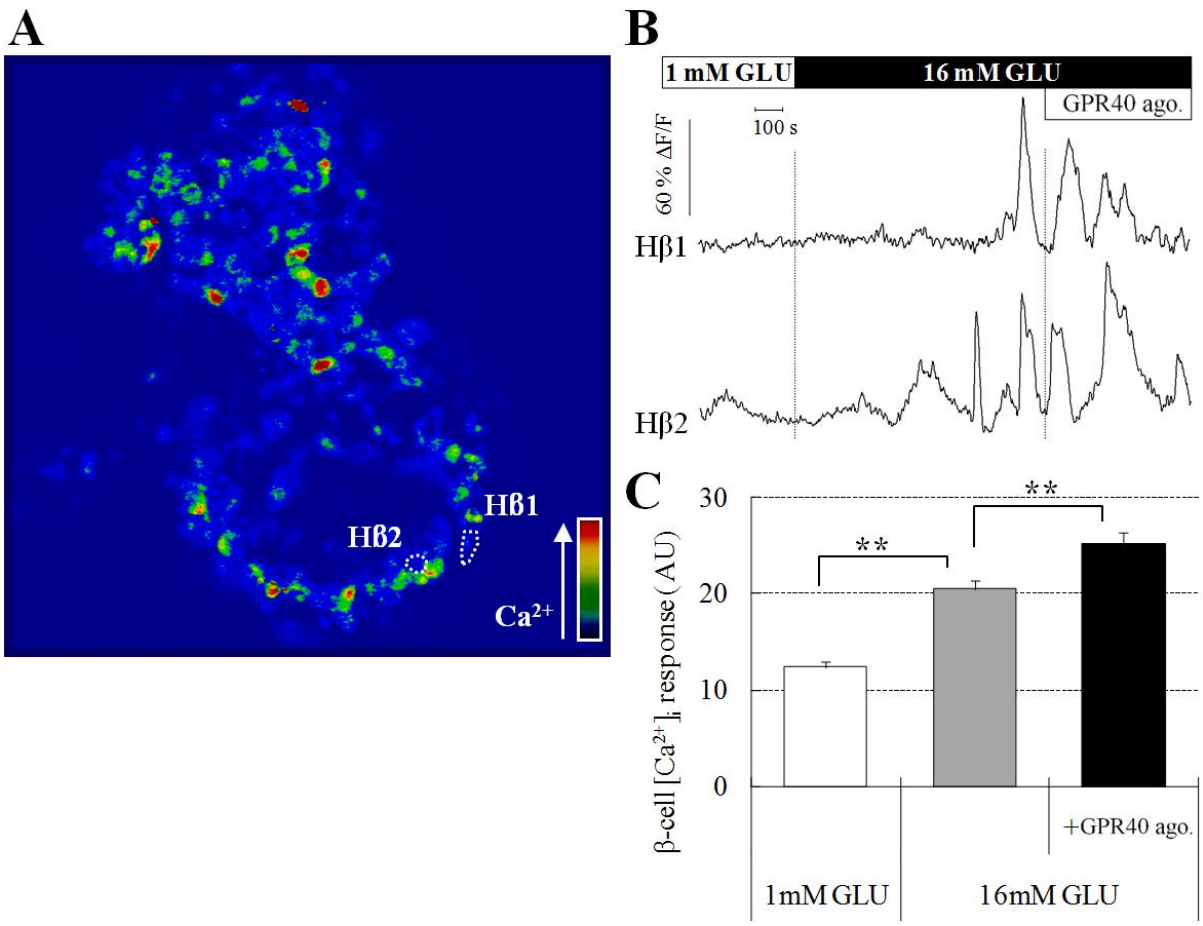

Fig. 23 Effects of GPR40 agonist on the intracellular Ca^{2+} response of single β- and α-cells within intact human islets

(A) Color image of human islet located with the Ca^{2+}-sensitive dye Fluo-4 at the beginning of Ca^{2+} recording. (B) Records of fluorescence intensity versus time from the cells indicated in panel A. Hβ1, 2 are representative $[Ca^{2+}]_i$ response from β-cells exposed to 1 mM glucose, 16 mM glucose, and 16 mM glucose plus 3 µM GPR40 agonist as indicated above the traces. (C) Summary of the $[Ca^{2+}]_i$ response from 146 single β-cells within 15 independent islets, expressed as mean ± *SEM*. ****** $p \leq 0.01$.

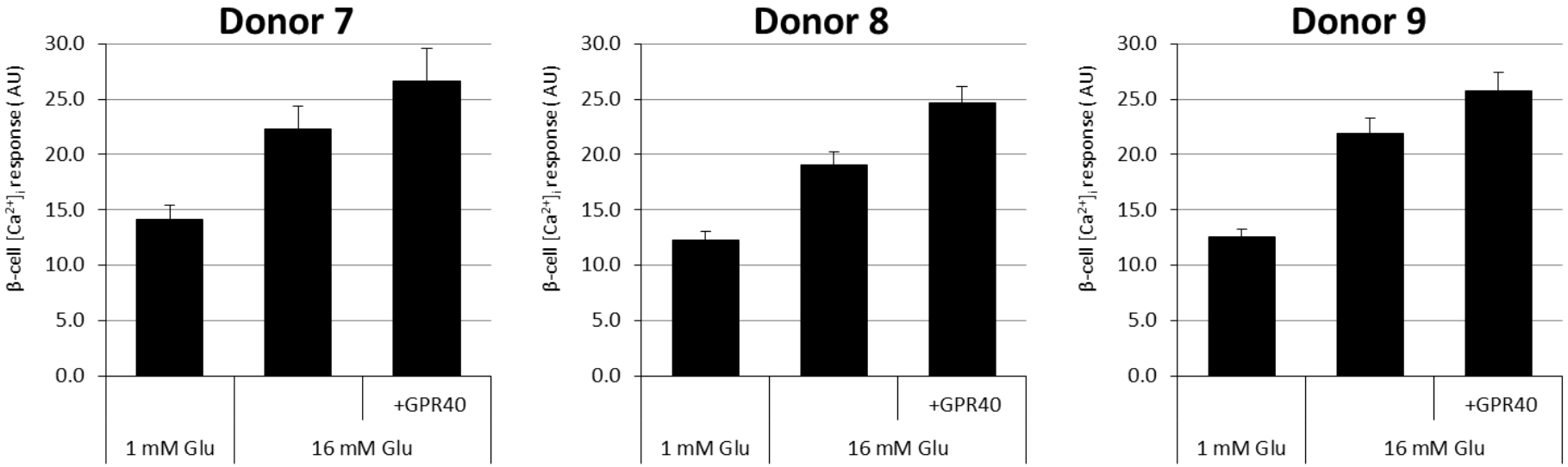

Fig. 24 Individual data of $[Ca^{2+}]_i$ response to 3 µM GPR40 agonist in three non-diabetic donors

The data are collected from 63 β-cells from 6 islets from donor 7, 8 and 9, respectively. Data are expressed as mean ±*SEM* (n=63).